UNIVERSITY OF OSLO
Department of Informatics

Power Harvesting Microelectronics

Master thesis

Trygve K. Halvorsen

2nd May 2008

Abstract

Wireless communication is increasingly popular due to the human urge to be independent and move around without being restricted by wires. With this trend come several challenges regarding both data transmission and how to power the wireless tag. This thesis addresses some of the key aspects of power harvesting, explores power harvesting capabilities in nanometer technology, but also consider different energy sources and discuss their adaptability to wireless identification tags. This thesis will also present a novel charge pump, with improvements using the back-gate or well of MOS devices. The possibilities to improve efficiency, as well as sensitivity, are discussed, and simulations, measurements and discussion of the results are provided at the end. The technology used is 90 nm CMOS.

Abstract

Preface

During the past five years I have attended the Master's Degree Program in Microelectronics at Department of Informatics, Faculty of Mathematical and Natural Sciences, University of Oslo. This thesis is submitted as a part of this program and concludes my work with the degree Master of Science. It was initiated in November 2006, and concluded in May 2008.

The work has been interesting and challenging in many ways, both due to the approach to the subject and the subject itself. The main focus has been the production of a chip in 90 nm CMOS technology and simulations and measurements in this regard.

I would like to thank my supervisor Tor Sverre "Bassen" Lande for his guidance and encouragement, driven by his passion for the subject and the genuine interest in my work. I would also like to thank my co-supervisor Håkon A. Hjortland, which has been helpful and extremely valuable to my work, and especially to the submissions of the scientific papers. And for a great deal of help with PCB layout and measurements, my gratitude goes to Håvard K. Riis.

Next I would like to express my thanks to my closest classmates Svein and Håvard. To Svein for his cooperation with the chip manufacturing process, and to Håvard for his expertice within the world of LaTeX and linux.

The great atmosphere among my fellow students at lab has been both a professional and social inspiration and has made the last two years cheerful and productive.

And last, but not least, thanks to Sigrid for all the motivation.

Oslo, April 2008

Trygve K. Halvorsen

Contents

List of Figures

List of Tables

Chapter 1

Introduction

1.1 Motivation: The wireless world

In the 70's, it was unimaginable for people to communicate with someone or something, without being attached to the network physically. Now, 30 years later, the term "wireless" has become a word everyone understand and can relate to, and even use to describe their own lifestyle. Picture, sound, video and other types of information are broadcasted, not just by big companies, but also from household computer systems. This wireless way of living raises countless possibilities, but also quite a few challenges. Security, adequate processing of personal data and ethical aspects are some, but the technology itself also has to meet the demands of an exacting trend.

Many of these technological challenges are power related. With the introduction of identification tagging like Radio Frequency Identification (RFID) to the commercial market, the battery has lost its acceptance level. The consumers expect small devices, like road toll tags, to have unlimited lifetime in some "magical" way. It is no longer considered outstanding, when devices are wireless and working.

As we can read in chapter 2.1, the history of the wireless identification technology has moved fast forward and some very interesting aspects are decreasing sizes, costs and increasing number of areas where the technology is used. To help this trend carry on, the power consummation and supply voltage will need to change dramatically. Supply voltages are pushed down to hundreds of millivolts, and the tags are becoming so small that embedded batteries not longer are a trivial part of the system. This, together with longer lifetime, means that power transmissions from the base station or reader to the tag are becoming more and more important. Tags without batteries, called passive tags, are used commercially today, but with very limited use. This type of tags are restricted to very short range systems, and for ranges above 0.1 m tags with batteries, called active tags, are preferred.

This work will investigate different power sources and design low power circuits for power supply purposes, with wireless identification systems in mind. RFID is today used to describe all wireless system that identify items in some way, and has become a quite vague term. This thesis is not exclusively concentrated around the RFID technology, but more around the subject RFID as the term is used today, as a common denominator for all systems using wireless tags.

1.2 Previous work

Since power harvesting is a huge subject there are many publications available, and a selection of these articles and books are used as background material for this thesis. As a guide to general passive wireless communication, the work of Vipul Chawla [Chaw 07] and Dr. Jeremy Landt [Land 01] have been valuable sources. Another source of information that can be mentioned is the seminar "RFID i næringslivet, status og trender"' [RFID 07], which was a great inspiration for the background research on the commercial aspects of RFID. The circuit design purposed in chapter 5, which is the main part of this work, is based on the discoveries of John F. Dickson [Dick 76], but the modification to a cascode charge pump is inspired by Karthaus and Fisher's [Kart 03] article from 2003.

1.3 Thesis outline

This thesis starts with presentation of the history and basics of wireless identification technology, frequency calculations and transmission methods. Further, the main part of the thesis is the design of a novel Radio Frequency (RF) charge pump, followed by the data from the measurements. A review of three different alternative energy sources composes the last chapter. The paper written about the charge pump is enclosed in the back of the thesis, and describes the charge pump in detail.

- Chapter 1 gives a short introduction to the subject, previous work, why this subject is chosen and this outline of the thesis.
- Chapter 2 presents the history of wireless identification and RFID and some examples of specific systems using this technology.
- Chapter 3 describes the basics behind the technology, a overview of certain frequency bands and a link budget.
- Chapter 4 presents various transmission methods used by wireless tags and communication systems.

- Chapter 5 is the part of the thesis where a circuit is designed and fabricated.
- Chapter 6 presents the measurement data extracted from the chip designed in chapter 5, and discusses the collected data.
- Chapter 7 reviews different alternative energy sources, both conventional and more experimental. A comparison of these follows at the end of the chapter.
- Chapter 8 summarizes the work, and give some suggestions to future work.
- The appendixes, A and B, contains figures of the charge pump and Printed Circuit Board (PCB).
- The paper written about the charge pump is enclosed in the back.

Chapter 2

Background

To get an understanding of the subject we first have to take a look at the history of wireless identification.

2.1 History

When looking back on the history of communication using reflected energy, the subject is quite big. It spans from passive filter tags to radar technology, and is applicable on several different areas. The idea of using radio backscattering to identify objects was used as early as pre-World War II, and the technologies behind were described even earlier.

We can say that RFID and wireless identification was born during the World War II. The Germans discovered that the reflected radio signal would change if pilots rolled their planes returning to the their home base. This simple method, at least technological simple, gave the base the opportunity to tell that these planes were German and not allied aircraft. Further, the Royal Airforce (RAF) also had a way to identify friendly planes called Identification Friend or Foe (IFF), invented in 1939. The IFF systems used coded radar signals called Cross-Band Interrogation (CBI) to trigger the friendly aircraft's transponder automatically when entering the radar zone. When the friendly aircraft "answered" at a certain frequency, the planes appeared brighter on the radar screen that other aircrafts.

At the end of this war, in 1946, Léon Theremin invented an espionage tool for the Soviet Union. This device retransmitted incident radio waves with audio information and the vibrations of the sound waves made a diaphragm move. This slightly altered the shape of the resonator, which modulated the reflected radio frequency. The listening device of Theremin can hardly be classified as a RFID tag, but still is considered as the first known RFID device, or at least the predecessor to the modern RFID tag.

In 1948 Harry Stockman published his paper "Communication by Means of Reflected Power" [Stoc 48] which turned out to be an important

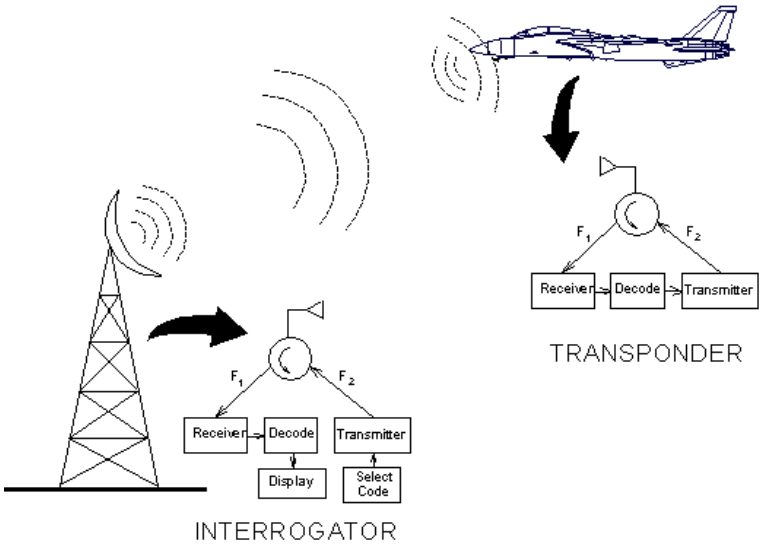

Figure 2.1: The basics of “Identification Friend or Foe”

article in the development of RFID. Amongst other things, Stockman predicted that "Considerable research and development work has to be done before the remaining basic problems in reflected-power communication are solved, and before the field of useful applications is explored." With this words, the foreseeing Stockman stated an allegation that is just as relevant today. Problems regarding reflected power are still researched, and with the progress of this research, the field of useful applications is expanding.

In the 1950s and 1960s the advances in radar and RF technology continued, and several papers on how to use RF energy to identify remote objects were written. A commercial breakthrough was the introduction of anti-theft tags in retail stores, which was the start of what is now known as Electronic Article Surveillance (EAS). EAS has been, and still is, a major part of the RFID technology and will be further explained in chapter 2.2.1 on page 10.

In the 1960s inventors also started to see the possibilities the technology offered, and several more or less usable inventions was born. Robert Richardson’s article about “Remotely activated radio frequency powered devices” from 1963 and Otto Rittenback’s “Communication by radar beams” in 1969 are two important works from this period. Richardson’s article describes a device that can rectify a coupled energy from an interrogator’s EM field, and transmit signals at a harmonic frequency of the received signal. These early RFID systems mainly used well known transmission methods, like radar technology, altdough in another scale. Still the inventions were very innovative, and during this period this trend also helped other branches of the telecommunication industry to evolve.

Near field devices were also popular in this period, and the inductive link got reborn, this time in the commercial arena.

The 1970s showed the world RFID research laboratories and a great deal of developmental work. Developers, inventors, companies, governments and especially academic institutions were actively working with RFID technology, and several research laboratories were founded. Amongst the institutions researching RFID in the 70s were the Los Alamos Scientific Laboratory, Northwestern University and the Microwave Institute Foundation in Sweden some of the most influential. Large companies like Fairchild and Radio Corporation of America (RCA) (now Thomson SA) started to develop RFID technology and in 1973 Raytheon launched the "Raytag". The Raytag was the first device used for animal tagging to track migration pattern, and was soon to be followed up by Richard Klensch of RCA and his "Electronic identification system" in 1975. In 1977 the "Electronic license plate for motor vehicles" was developed by Fred Sterzer (RCA). Vehicle scanning systems in big scale were tested in the 70s, and one example of this was when the Port Authority of New York and New Jersey tested various systems from General Electric, Westinghouse, Philips and Glenayre. These systems were promising, but not yet adequate. During a conference held by the International Bridge Turnpike and Tunnel Association (IBTTA) and the United States Federal Highway Administration in 1973, the conference concluded that there was no national interest in developing a new standard for electronic vehicle identification. Once again, the technology was not ready to hit the market.

In the 1980s the same trend continued, with further commercialization and new patents rolled out of the research facilities. While the scientists in the United States aimed towards transportation and personnel access, the research in Europe focused on short-range tracking of animals, industrial tracking, factory automation and electronic toll collection.

In 1987, 14 years after the US rejected the technology, the electronic toll collection was launched. By the end of October 1987 the first RFID-based toll collection system was up and running in Ålesund, Norway. This was a big breakthrough for RFID, since this system showed good quality, even in commercial use. This system was implemented by the Swedish company Combitech AB, which later was bought by Austrian Kapsch. Not long after this breakthough RFID based toll stations were to be seen in toll roads in Italy, France, Spain and Portugal too. This trend was soon to be adopted across the world and "across the pond" the Association of American Railroads and the Container Handling Cooperative Program were active with RFID initiatives. The Port Authority of New York and New Jersey picked up were they had left in the 70s, and began commercial operation with RFID. This process started with tagging of buses going through the Lincoln Tunnel, but expanded quickly to other areas.

RFID was now used in several arenas and this use prompted a need

for standards. During the 1990s the standardization was mainly controlled by the International Standards Organization (ISO) and International Electrotechnical Commission (IEC). ISO is an international standard-setting organization with representatives from nearly all national standards organizations in the world. The organization with headquarters in Geneva, Switzerland, was founded in 1947 and declares world-wide industrial and commercial standards. ISO is a non-governmental organization, but still the decisions made by this organization often become law across the world.

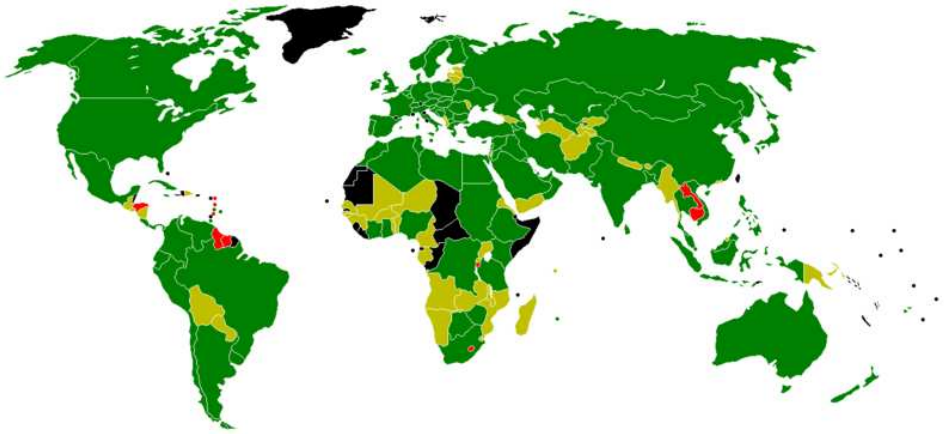

Figure 2.2: ISO members are marked by a green color, correspondent members by yellow, subscriber members in red and non-members are shown in black. (Courtesy of the International Organization for Standardization)

IEC is a similar non-profit, non-governmental global organization, and works with standards for electrical, electronics, and related technologies. More specific, the IEC covers a wide range of technologies such as batteries, power generation, transmission and distribution, home appliances and office equipment, fiber optics, semiconductors, solar energy, micro- and nanotechnology and marine energy. Some of the "famous" standardizations are color marking of resistors, capacitors and inductors, known as the electronic color code (IEC 60062), the standardization of the RJ45 connector (IEC 60603-7), the VHS video tape cassette system (IEC 60774) and semiconductor devices (IEC 60747). The IEC collaborates with the Institute of Electrical and Electronics Engineers (IEEE), the ISO and the International Telecommunication Union (ITU). IEC, founded in 1906, counts more than 130 countries and 69 of these are active members.

The standardization of animal tracking devices (ISO-11784 and ISO-11785) and contactless proximity cards (ISO-14443), were the first standardizations that regarded RFID. With standardization came the possibilities to cooperate across systems, and the first cooperative RFID system was a system based on the Title 21 standard installed on the Kansas turnpike. This

system had readers that could also operate with tags from the Oklahoma toll systems. This made it much easier for the consumers, since only one tag was needed when travelling between the states. Georgia soon followed up with readers that could communicate with the new Title 21 tags as well as the existing tags, and the standardization proved to be a success. This was taken futher by the 12-county Dallas-Fort Worth-Arlington metropolitan area. They used a single tag, titled TollTag, to pay tolls on the North Dallas Tollway, parking payment at the Dallas International Airport, Dallas Love Field airport, downtown parking garages and to access gated communities and business facilities.

The interest both in Europe and the US was now turned once again towards access and control systems, and both microwave and inductive technologies were used in this purpose. Texas Instruments developed their TIRIS system with success and the TIRIS was used in cars and trucks to control starting of the engine. This system, together with other similar systems, developed new applications. Fuel dispensing, ski passes, and vehicle access were some of them.

A milestone in the history of RFID came in 1996, when RFID became standardized as a data carrier by the Article Number Association (ANA) and European Article Numbering (EAN) groups. The EAN International and the Uniform Code Council (UCC) (Now both known as GS1 together with the Electronic Commerce Council of Canada (ECCC)), adopted in 1999 a UHF frequency band for RFID and later founded the Auto-ID Center at the Massachusetts Institute of Technology (MIT). The Auto-ID Center was the predecessor to Auto-ID Labs and EPCglobal, and later developed the Electronic Product Coding (EPC), which is a standard for electronically labeling products with RFID. EPC will be further discussed in chapter 2.2.2 on page 13.

Another breakthough in this decade was the advances in silicon technology, which made silicon based RFID tags cheap and reliable. Useful microwave Schottky diodes were now possible to fabricate with regular CMOS integrated circuits, and this led way for construction of microwave RFID tags on a single integrated circuit. Lower costs and risks regarding hardware failure made it possible to run large-scale projects. Tags became cheaper and smaller, and could be used to tag smaller and cheaper items, like the products sold at Wal-Mart. Wal-Mart Inc., an American chain of large, discount department stores, launched in the early 2000s one of the largest and best known RFID projects until now. Tagging that many items is a demanding job. To make this project doable, they also demanded their suppliers to implement this system, and at the Retail Systems Conference in June 2003 in Chicago, they presented the system. The release of the first EPCglobal standard followed in January 2005. Wal-Mart, which was the largest public corporation in the world by revenue in 2007, now have more than 1000 stores with EPC RFID standard implemented.

Table 2.1: The RFID History summarized

Decade	Event
1940 - 1950	Radar refined and used, major WWII development effort. RFID invented in 1948.
1950 - 1960	Early explorations of RFID technology. Laboratory experiments.
1960 - 1970	Development of the theory of RFID. Start of applications field trials.
1970 - 1980	Explosion of RFID development. Tests of RFID accelerate. Very early adopter implementations of RFID.
1980 - 1990	Commercial applications of RFID enter mainstream. First electronic road toll collection.
1990 - 2000	Emergence of standards. RFID widely deployed. RFID becomes a part of everyday life.

2.2 Systems and applications

The possibilities with wireless technologies are many, and as we have seen during the past 50 years, the number of areas where RFID and similar systems are used, expands rapidly. Not only systems developed for a single purpose, but also standards. In this chapter a few specific systems from the most common areas will be described to give an understanding of the way large RFID systems and standards works. EAS uses different types communication methods and is a good place to start when entering the world of energy harvesting and wireless tags.

2.2.1 Electronic Article Surveillance

EAS was one of the first commercially used systems that identified objects using RF or inductive link, and is an important part of the security system of a retail store. The technology is used to identify items or merchandise when they pass through the exit or a gated area, and is implemented to prevent unauthorized removal of items from a store, library or other places where shoplifting occurs. The systems consists of three components; tags or labels (sensors) that are attached to merchandise, deactivators or detachers to use by the clerks, and finally detectors that create a surveillance zone at the exits. There are several different EAS systems available on the marked, but common for them all is that an EAS tag or label is attached to the item. When the item is purchased or borrowed, the tag is detached or deactivated and the item can be carried out of the store without setting off the alarm. By using an EAS system, it is not necessary

to lock the product away, which makes it easier for the consumer to review the product. The cost of tagging all the products is also decreasing, as many suppliers now build the tag into the product at the point of manufacture or packaging. This saves both money and time in the stores and makes it harder for shoplifters to remove the tags.

The choice of which communication method to use depends on many factors. The technology affects the ease of shielding, the visibility and size of the tag, the rate of false alarms, detection rate and cost. Even if the different methods seem equal to the untrained eye, todays EAS systems can be divided into four different categories:

- Electromagnetic
- Acoustomagnetic, also known as magnetostrictive
- Radio frequency
- Microwave

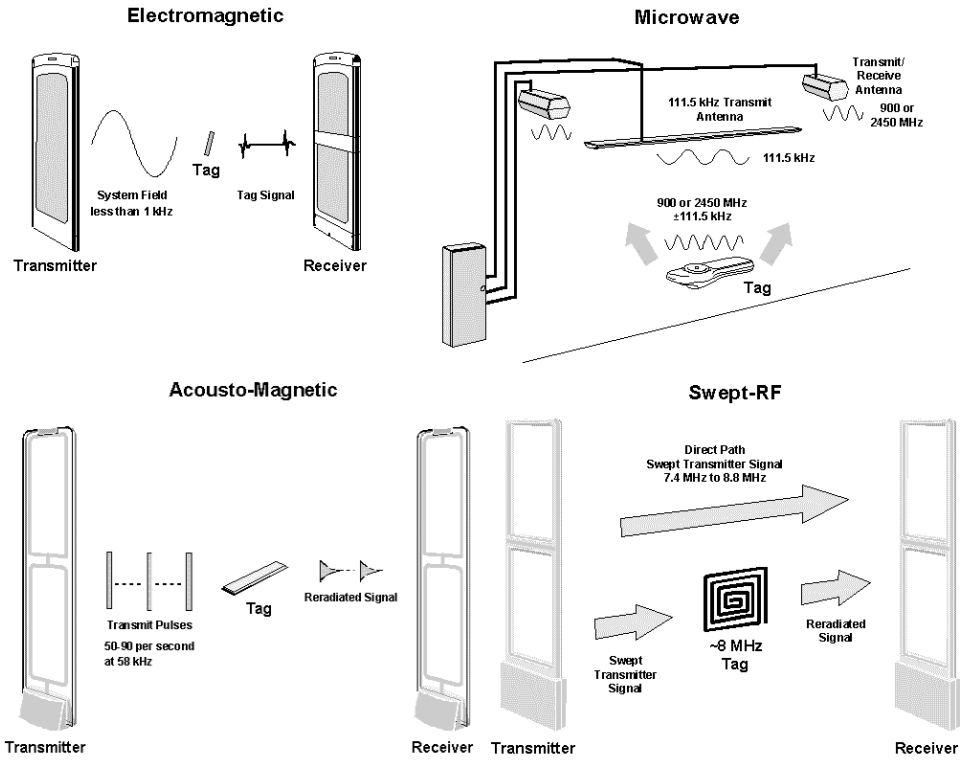

Figure 2.3: Different types of Electronic Article Surveillance. (Courtesy of Association for Automatic Identification and Mobility)

Electromagnetic

The electromagnetic EAS system uses the detectors to generate a low frequency electromagnetic field, in the frequency range of 70 Hz to 1 kHz. This field will change strength and polarity when repeating the cycle from positive to negative and back. And with each half cycle, the polarity of the magnetic field changes. This alternating magnetic field created by the transmitter will affect the tag, and this sudden change in the magnetic state will generate a signal from the tag. This signal will have lots of multiples of the fundamental frequency, also called harmonics of the original frequency. The reader will then detect these harmonics by frequency, strength and time in relation to the transmitter.

Acoustomagnetic

Acoustomagnitic EAS is quite similar to the electromagnetic, but operates at a higher frequency. The transmitter sends a signal at 58 kHz in pulses, and power the tags in the surveillance area. The tag works like a tuning fork, and replies to the reader with a frequency close to the transmitter signal. In order to detect the tag that replies at the same frequency as the transmitter is using, the reader have to listen for tags between the pulses of the transmitter when the transmitter is off. If a signal with this frequency is detected when the transmitter is quiet, the alarm is activated.

Swept radio frequency

This method differs from the magnetic methods because the frequency is not fixed, but the RF - EAS sweeps the frequency between 7.4 MHz and 8.8 MHz. This signal energizes the tag, which in this case is often more like a sticker with copper wires called a label. This label contains a capacitor and an inductor, and the components are able to resonate when connected together in a loop. The frequency which the transmitter operates at, has to be matched with the component values in the label. The emitted signal from the label can be distinguished by the reader in order to detect the label.

Microwave

As figure 2.3 on the preceding page shows, this type of EAS look quite different than the other three. The system is composed of a transmitter, a synchronous receiver, a microprocessor-controlled detector and an alarm. The transmitter generates two different signals in the surveillance area, one high frequency carrier signal and one low frequency signal. The high frequency signal is in Europe between 2402 MHz and 2486 MHz, and in North America between 902 MHz and 906 MHz. This is to

avoid interference with other systems, since the frequency regulations are somewhat different in different parts of the world. The low frequency signal is a modulation signal and operates at 111.5 kHz. This signal is a non-propagating, electrostatic signal to limit the RF field to the surveillance zone. The tag in this system consists of a microwave diode and an antenna. This antenna is tuned to receive the signals from the transmitter and when the tag is in the surveillance zone, the tag combines the two signals and reflect the combined signal to the receiver. The modulation of the high frequency signal with the low frequency signal is amplified by the receiver and compared to a reference signal to make sure when to activate the alarm or not.

2.2.2 Electronic Product Code

The barcode has been a key part of product labelling since Joseph Woodland and Bernard Silver patented the first bar code system on October 7, 1952 [Shep 04]. Almost every product in the world is identified with a barcode, even if it is a carton of milk at the grocery store or spare parts at a warehouse. The main drawback with barcodes is that they have to be visible to be read. Dirt, rifts, interference with other objects or wrong alignment can cause reading problems. With the introduction of RFID to the commercial market, the barcode got competition. The advantages with RFID over barcodes are many, but both cost, security and complexity issues have held RFID back. Now that the prices have decreased and RFID has become more mainstream, it has replaced barcodes in several arenas. And as described in chapter 2.1 on page 5, Wal-Mart's implementation of RFID it probably the most famous example. With widespread use of RFID solutions to identify items, standards were needed.

EPC is a group of coding schemes created to replace the bar code with time, which was created by MIT at the Auto-ID Labs as a low-cost method of tracking goods using RFID. It is designed to work like the barcode, guaranteeing uniqueness and to fit various industries and products. In comparison to the barcode, the EPC tags are designed to identify each item manufactured, whilst the barcode only identify the manufacturer and class of products. The EPC standard, which today is managed by the EPCglobal, will probably become the global standard for RFID, and a core element of the proposed EPCglobal Network. The reason why some many store chains and industries are planning to, or already are using EPC, is that RFID also can be used as a tracking device all along the supply chain. The current EPC version is 96-bit and contains information about the manufacturer, the product class and a specific serial number that identifies that specific object. This gives the buyer the opportunity to follow the product all the way back to the factory and even implement extra functionality like temperature-sensors on frozen products. All this can be logged, the supply

Figure 2.4: RFID used to track and identify items in every step of the logistic process. (Courtesy of DC Logistics)

chain can be made more effective and the facts regarding products that are "dead on arrival" are easier revealed. This can be done across borders and companies, if your partners also use EPC.

The future challenges for EPC based RFID are the technology. Tags have to be cheaper, the reading distance longer, and the ability to read several tags at once will have to improve. The promising EPC standard is already existing worldwide, but as we have seen throughout the history, the technology will have to mature before the standards and ideas can work commercially.

2.2.3 AutoPASS

There are many different electronic road toll collection systems in use around the world, but we will now take a closer look at the one used in Oslo, Norway. The development work of the Autopass system started in 1998, as the successor to the Surface Acoustic Wave (SAW) tags which is described in chapter 4.4 on page 38. Some of the motivation for a new system was that the frequency previously used, 856 MHz, was under concession by the Norwegian Post and Telecommunications Authority (NPT) for digital TV. The new system, AutoPASS, was launched late 1999 and operates at 5.8 GHz with semi-active tags (See chapter 3.1). Since the start in 1999, the 3. generation toll system is implemented at almost 30

other toll roads, making the system one of the most modern and popular toll systems in Europe.

Figure 2.5: With AutoPASS you can pass the toll collection even at high speeds.

The tags used in the AutoPASS system are using Amplitude Shift Keying (ASK) and Phase Shift Keying (PSK) (see chapter 4.2 on page 34) for receiving and transmitting respectively, has a max reading distance of 10 meters and an expected battery lifetime of about 5 years. The European Committee for Standardization/Comité Européen de Normalisation (CEN) is currently working on a European standard for electronic road toll collection and AutoPass will be a part of this standard. The idea is to make it able for all Europeans to use the same tag in every toll road across Europe. For AutoPASS, this partnership is today limited to the Nordic countries, and the AutoPASS tag can be used at several large toll roads and bridges in Sweden and Denmark in addition to most Norwegian toll roads.

Chapter 3

RFID and wireless power

In order to design a working RFID tag, the way of powering the tag is an important issue. The choice of energy source and transmission method is crucial and strongly depends on the use and environment of the tag. Many different solutions have to be considered, and operating radius, fabrication costs and size are usually the factors that will point out which type of tag to use. RFID tags can be classified into three main categories; active, semi-active or passive.

3.1 Different RFID types

3.1.1 Active tags

Active RFID-tags completely rely on a battery to operate, and therefore can transmitt data in the absence of an RFID reader or an external energy source [Shep 04]. This type of tags are widely used in various applications, but are the most expensive type of tag because of the battery, and also because active tags are often more complex in design. There are many fields of usage where an active tags can be used, but the use is limited as the battery will need replacement. If the battery lifetime is a problem, i.e. in medical implants, a semi-active or passive tag can be used.

3.1.2 Semi-active tags

Semi-passive tags also have an embedded battery to power the tag, but operate somewhat differently. Normally, this battery is only activated when the tag is in the range of a reader. This will result in longer battery lifetime since the tag is not constantly transmitting data. Still, semi-active tags operate at long ranges, but the size of the tag is often conciderable larger than passive tags. A well known example of semi-active tags used commercially is the AutoPASS system, which is used as a payment

Table 3.1: Compression of the different types of RFID-tags.

	Battery	**Range**	**Cost**	**Lifetime**
Active	Yes	Long	High	Very limited
Semi-active	Yes	Long	High	Limited
Passive	No	Short	Low	$\simeq$unlimited

system for toll roads around the world, from Norway to Australia. (See chapter 2.2.3 on page 14) The battery lifetime of todays AutoPASS tags is around five years, but the battery is replaceable.

Figure 3.1: AutoPASS is used successfully in road tolls but has limited lifetime.

3.1.3 Passive tags

A passive RFID tag requires no internal power source or embedded battery, but harvest the energy from the reader or the environment. This can be either inductive, like in Skipass (figure 3.2 on the next page), or the tag can receive its energy from a high frequency signal, like WLAN, through an antenna. This type of tag is the least expensive, but it also have very limited range compared to the battery-powered alternatives. Passive tags are usually non-programmable, and only contain the code of identification which the tag transmits in close proximity of an energy source or reader. The advantages of passive tags, are that these tags are usually smaller in size and cheaper to manufacture.

With each one of these different types of tags, we can find both advantages and drawbacks, and a combination of only the advantages would of course be the ideal thing. To make the scenario realistic, the financial aspects will be taken into account, because RFID-products need to have a low unit-price to be profitable in the commercial arena, which will expand the possibilities of the tag significantly. Hence the active and

Figure 3.2: Skipass is a short-range passive RFID-tag. (Courtesy of Trovan Inc.)

semi-active technologies are not an option in this thesis, because of the size of the tags and expenses related to the production.

These passive tags without batteries will still need power, and in the next chapter various methods for wireless power transmission are considered for use with passive RFID technology.

3.2 Wireless power

The main problem with passive RFID tags is what the name implies. They are passive. Since they have no batteries, the challenge will be gathering enough energy and to minimize the energy consumption of the hardware.

The efficiency of an energy transferring system is defined as the percent of the energy sent which reaches the destination. When transferring energy through a wire, the conduction path has a low resistivity and the efficiency is high, but this is different when working with wireless signals. Wireless transmission of energy is usually not very efficient because most of the energy which is sent misses the receiver, or is lost as heat. The energy is much harder to guide than with a regular electrical wire, and this is why the choice of transmission method is important in order to succeed in powering a passive tag. Although it is very hard to transmit energy at long ranges, we can find examples of large scale projects involving wireless power. One is the futuristic project of National Space Agency (NASA), called Space Solar Power (SSP). This can probably be the largest man-made energy transfer in the world if ever launched, literally speaking. This project involves launching a Solar Power Satellite (SPS) out in high earth orbit, to transmit solar power back to earth using microwave power transmission. The advantages of collecting the solar power in space is that the solar cells is not affected in any way by weather, nights or seasons. In other words; a clean, environment friendly way to harvest energy, for

consumption on earth. A good idea at the drawing board, but for the time being the launch and maintenance costs are way to high for this project to succeed. The SPS transmit by the use of Microwave Power Transmission (MPT), which will be discussed later in this chapter. At the other end of harvesting technology, we find everyday electronics, like wireless charging of electrical toothbrushes and wireless powering of electric water boilers. Short range wireless power is used in many different applications, and we use products with this type of power conduction more often than we think.

We will now take a look at some different methods for wireless transmission, and first out is a common technology used for short range wireless energy transmission, called an inductive link.

3.2.1 Inductive link

With the invention of the electromagnet in 1825, William Sturgeon invented a main ingredient of the inductive link [Stur 08]. The other ingredient was discovered by Michael Faraday in 1831, and was called the electromagnetic induction [Fara 08]. Electromagnetic induction is that a changing magnetic field can induce an electrical current in an adjacent wire, and can be demonstrated by the use of two electromagnets. The first person to do this was Nicholas Joseph Callan in 1836, and with this discovery he showed the world the inductive link [Case 82]. Callan's induction coil apparatus consisted of one insulated coil he called the primary winding, and another longer one he called the secondary winding, both with an iron core. When he connected a battery to the primary winding, it induced a voltage in the secondary that he could use to light a lightbowl. In figure 3.3 on the facing page an inductive link is shown. A current is introduced in one coil which creates a magnetic field. If another coil is in the proximity of the first coil, the magnetic field induces a current in the second coil. Farraday's law of induction states that the induced electromotive force in a closed loop is directly proportional to the time rate of change of magnetic flux through the loop. In other words; when a current is introduced in the primary winding, the magnetic flux will change, and the changing field will induce an electromotive force in the secondary [Fink 03].

$$\mathcal{E} = -\frac{d\Phi_B}{dt} \cdot N$$

where $\mathcal{E}$ is the electromotive force in volts, Φ the magnetic flux in weber, N is the numbers of windings and t is the time.

Although Callan did not use this discovery in commercial use, the technology is now used in everyday applications like charging electrical toothbrushes. The downside of this technology is the range. For long range devices, a bigger coil is needed. I.e. a Skipass operates on just a few centimeters and still uses a coil just as big as the card. This is a well

proved technology, but not ideal for RFID tags. It works adequately in ticket systems and for powering home electrics, but the size would then be larger than tolerated if non-reusable tags had the physics of a credit card.

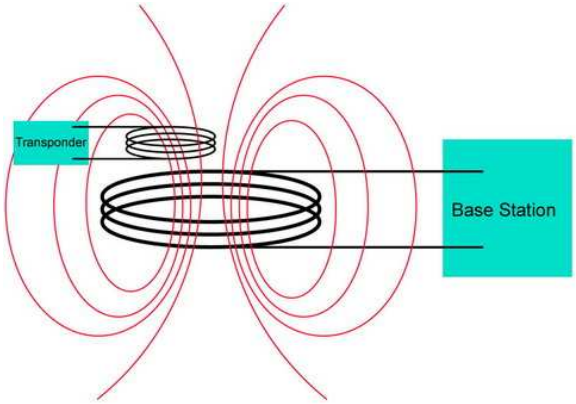

Figure 3.3: Basically how an inductive link works

To transmit over a longer distance, other methods like microwave power transmissions can be used.

3.2.2 Microwave Power Transmissions

The term microwave refers to electromagnetic energy having a frequency higher than 1 GHz, corresponding to a wavelength shorter than 30 cm. In other words, the microwave range includes UHF, SHF and EHF signals. This frequency range is used in MPT, which is the use of microwaves to transmit power wireless over a long distance. This is of course not commonly used by small scale devices like RFID, but promising in larger projects and can tell us something about the future of wireless power transmission. To understand this futuristic technology, we first have to look at some history.

In 1961, William C. Brown published the first paper on MPT [Brow 65], and three years later, he demonstrated it by flying a microwave-powered helicopter. The helicopter was only powered by a microwave beam using 2.45 GHz, which is within the frequency range of 2.4 GHz - 2.5 GHz reserved for the ISM applications of radio waves (See chapter 3.3.2 on page 25). A power conversion device from microwave to DC, called a rectenna, was invented and used for this microwave-powered helicopter. MPT is a promising technology, and because microwave devices offer high efficiency of conversion between DC-electricity and microwave radiative power, MPT will probably be used more in power transmissons in years to come. Scheduled MPT projects are now using a phased array microwave transmitter to electrically steer the system using no moving parts. Another

advantage is the easy scaling to the necessary levels that a practical MPT system requires, but then the drawback is lower efficiency.

When working with microwaves, there are several aspects to consider along the way. Besides the challenges of the technology, there are regulations and safety issues to pay attention to. This apply to futuristic space projects as well as regular microwave ovens used in households. These kind of ovens follow strict regulations and have a very small leakage of microwaves, due to the Faraday cage which all ovens are equipped. This cage have a much smaller perforations in the mesh than the used microwave wavelength of 12 cm, hence most of the microwave radiation can not pass through the door, while visible light with a much shorter wavelength can.

Figure 3.4: The ADS mounted on a Humvee (Courtesy of The Joint Non-Lethal weapons program.)

To illustrate the impact microwaves have on humans and living creatures, we can take a look at the Active Denial System (ADS) of the U.S. army. The ADS, often referred to as "The pain ray", is a 95 GHz microwave transmitter used for crowd control. It works by directing electromagnetic radiation toward groups of people, and the microwaves heats the water molecules in the outer skin layers to around 55 °C. This causes the crowd "under fire" to feel a painful burning sensation, and heats in the similar way as a microwave oven. The ADS has a range of approximately 500 m, and is expected to be deployed in Iraq by the end of 2008. As expressed in several scientific communities, this is not a popular use of the powers of the microwave, but the developers claims, of course, that this type of exposure to microwaves will not give long-term health effects. Even if this

Table 3.2: Some of the ISM-bands within the EU

Frequency	Usage	Wavelength
900 MHz	GSM 900	33.3 cm
1800 MHz	GSM 1800	16.7 cm
2.45 GHz	Wireless LAN	12.5 cm
5.8 GHz	Cordless Phones	5.2 cm

is true, people trapped in a crowd can be exposed to serious pain or even have their limbs or eyes injured.

3.2.3 RF energy

In the term RF we will find all frequencies from 3 kHz to 300 GHz. Originally, RF was used to describe frequencies of alternating current electrical signals used to produce radio waves. Since high frequency systems have become more usual, this definition has become more and more vague. Above 1 GHz, the term is often used in the same settings as microwaves, hence this can be quite confusing. Now, the definitions are many, and to avoid confusion, this thesis will from now on only use the term RF. Radio Frequency, or Radio Frequency Power, is the most common term to use when discussing power harvesting at high frequencies.

When working with high frequency signals, like the ones in the gigahertz range, the energy of the signal is hard to get a hold on. There are different ways to capture high frequency energy like this, but the losses are often high and increases rapidly with distance. In other words; the attenuation in air is high.

To make a RFID-system with passive tags work in different types of environments, there always have to be signals available. When harvesting energy, the tag can either take advantage of existing signals, or get the energy through high frequent signals from the reader. A great advantage with these signals is that they are widely used in various applications, and therefore are available for harvesting in many environments even if they often are weak. Wireless Local Area Network (LAN) or cellphone signals can be used, but it depends on the application and power needs. If a generated signal is used, there are strict governmental limitations regarding the transmission of signals at these frequencies. Another advantage with such a high frequency is that the antenna size is inverse proportional with the frequency. At frequencies in the gigahertz range, the antenna size can be small enough to be embedded.

Other more experimental and alternative ways to power a passive RFID tag are discussed in chapter 7 on page 73, but first we will take a closer look at how to harvest energy from high frequency wireless signals. This is because frequencies of 900 MHz and 2.45 GHz are easy to generate and

even can be found "naturally" around the tag.

3.3 Frequency bands, calculations and measurements

First we will take a closer look at the 900 MHz and 2.4 GHz Industrial, Scientific and Medical (ISM) bands available for RFID use.

3.3.1 900 MHz ISM band

Around 900 MHz we find a popular frequency range for amateur radio, and in 1985 the “33 centimeter radio band” was born. The Federal Communications Commission (FCC) allocated 902 MHz to 928 MHz for Industrial, Scientific and Medical (ISM) devices. As part of that edict, the band was allocated to the Amateur Radio Service on a secondary basis. This means that hams can use the band as long as they accept interference from and do not cause interference to the primary user. “Ham“ is an informal term for an amateur radio operator, and the word "ham" was born in 1908 when the station call of the first amateur wireless station where operated by amateurs of the Harvard Radio Club. They were named Hyman, Almy and Murray, and named their station by combining their capital letters [Why 59].

5 years after the start, many mobile cordless phones appeared on the lower and upper ends of the 900 MHz band, phones that earlier operated at 46 MHz. When this band became over-crowded, the phones moved up in frequency, and now do Global System for Mobile communications (GSM) mobile phones share this bandwith with automatic vehicle monitoring systems and authorized U.S. governmental radio stations [ERC 04].

Unfortunately, this frequency band is not available for ISM applications in Europe at the moment, but outside Europe this band commonly used by RFID systems. The range of 868 MHz to 870 MHz is available in Europe for short range devices like RFID, and is often used as a substitute [Fink 03].

3.3.2 2.4 GHz ISM band

The 2.4 GHz band covers frequencies from 2400 MHz to 2483.5 MHz and is being used for an increasingly diverse range of applications and systems. The band is non-licensed for private users, but is regulated with regard to power levels which leads to a potentially low level of service quality when used in non-controlled environment with unpredictable levels of interference. This can be crucial to systems that are safety critical or public services where the quality have to be high at all times. Still the 2.4 GHz band has many advantages. The low frequency, relative to other communication band like the 5.8 GHz band, makes the it suitable for mobile communications. Another attraction is the global standardization, which makes it easier for international manufactures to design products that will work world wide.

Table 3.3: Users of the 2.4 GHz ISM-band

User type	Exempt from license
Military	No
Electronic News Gathering and Outside Broadcast	No
Public provision of Fixed Wireless Access	No
Radio LANs	Yes
Bluetooth	Yes
SoHo and Home networking	Yes
RF Identification Devices	Yes
Video applications	Yes
Microwave ovens	Yes
Sulfur plasma lighting	Yes

Table 3.4: The best known classes of the IEEE 802.11 standard

Standard	Launched	Medium	Channels	Theoretical throughput
802.11	1997	2.4 GHz	3	1-2 Mbps
802.11b	1999	2.4 GHz	11(13)	11 Mbps
802.11a	1999	5.6 GHz	12	54 Mbps
802.11g	2003	2.4 GHz	11(13)	54 Mbps
802.11n	No	2.4 / 5 GHz	3 / 12	100-540 Mbps

The users of the 2.4 GHz band are many (See table 3.3). The military in several countries pays big money for use of this band every year, and mainly use it for communication and identification reasons [Lees 00]. TV stations and broadcast networks uses the band for short range transmission of video. One example is coverage of sporting events, like transmission of live picture from a field camera (following bikes, skiers, golfers etc.) to a central unit or a recorder. This is called Electronic News Gathering (ENG), which also covers on-site news reporting. ENG can be very unpredictable in terms of timing and location and will in many cases have to be established quickly, with little or no time for frequency co-ordination and licensing. Other examples are Closed Circuit Television (CCTV), Fixed Wireless Access (FWA), Bluetooth and of course the IEEE 802.11 standard [Lees 00].

IEEE 802.11 is a set of standards for WLAN computer communication, developed by the IEEE LAN/MAN Standards Committee (IEEE 802). The standard includes both the 5 GHz and 2.4 GHz public spectrum bands, and is the one used by modern routers for wireless networks. The most common classes of the IEEE 802.11 standard are listed in table 3.4, and the ones used for WLAN are 802.11b and 802.11g.

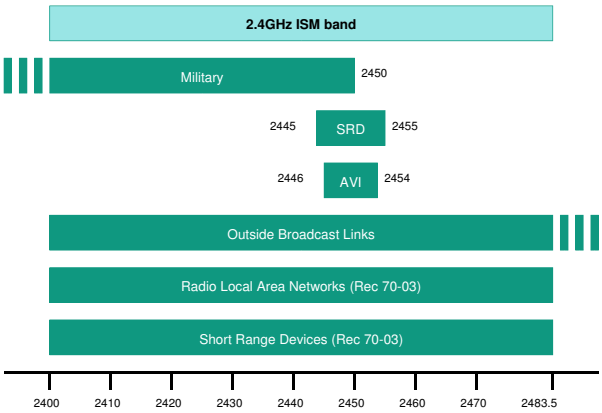

Figure 3.5: Users of the 2.4 GHz ISM-band. (Courtesy of Ægis Systems Limited)

To get a estimate of how much available energy that can be carried by a 2.45 GHz signal, and how much energy a passive wireless tag can harvest from it, a link budget is needed. In the calculation we use 2.45 GHz, because this is the center frequency of the ISM band. A link budget is the accounting of all of the gains and losses from the transmitter, through a medium (in this case; air) to the receiver. The link budget takes into account the attenuation of the transmitted signal due to propagation as well as the loss, or gain, due to the antenna. This budget gives a good indication although random attenuation such as fading is neglected.

3.3.3 Link Budget

A simple setup for received power:

$$ReceivedPower = TransmittedPower + Gains - Losses$$

To find all the gains and losses, both the transmitter antenna, the receiver antenna and all in between have to be included:

- RxP = received power (dBm)
- TxP = transmitter output power (dBm)
- TxG = transmitter antenna gain (dBi)

Table 3.5: Maximum allowed transmit power in 2.4 GHz ISM-band

Area	Allowed transmit power	Regulations
EU	4W	Indoor only
USA	4W	None

- TxL = transmitter losses (coax, connectors...) (dB)
- FSL = free space loss or path loss (dB)
- ML = miscellaneous losses (fading, body loss, polarization mismatch, other losses...) (dB)
- RxG = receiver antenna gain (dBi)
- RxL = receiver losses (coax, connectors...) (dB)

This gives us the following equation:

$$RxP = TxP + TxG - TxL - FSL - ML + RxG - RxL$$

The output power of the transmitter is, in this case, the maximum transmit power that is allowed at the 2.4 GHz ISM band. This is however not the same limit all over the world, although the 2.4 GHz ISM band exists worldwide, see table 3.5. In Europe and the US, the maximum allowed power output of a 2.4 GHz ISM radio is 30 dBm (1 W) before the antenna. If the antenna gain is included, the maximum power allowed is 36 dBm, leaves us with the maximum output of 4 W for indoor use in EU.

The transmitter antenna will have a amplifying effect, depending on size, type and direction. Since this is a controllable factor it will be, in the calculation, modulated as an isotropic antenna which has no gain or loss, regardless of the direction. The same applies for the receiver antenna. The largest loss in this budget will be the free space loss. This will be dominating relative to other transmitter and receiver losses, in addition the miscellaneous such as fading.

3.3.4 Free space loss (FSL) and Friis' formula

The loss through the medium (Free Space Loss (FSL)) is an important factor. This is a way to find the loss in vacuum, and since the difference is not that significant at one meter radius, it can be used as a good estimate for transmissions through air. Friis'-formula is the most common formula to use:

Friis' formula:

$$FSL = \left(\frac{4 \cdot \pi \cdot R \cdot f}{c}\right)^2$$

Since we modulate our antenna as an isotropic antenna, we can use a more simple form to calculate the loss with transmitter/receiver-distance r, and frequency f [Fink 03]:

$$FSL(dB) = 20 \cdot \log_{10}(d) + 20 \cdot \log_{10}(f) - 147.5 \text{ dB}$$

If the relevant frequency (2.45 GHz) and radius (1 m) is inserted, the FSL will be:

$$FSL(dB) = 20 \cdot \log_{10}(1) + 20 \cdot \log_{10}(2.45 \cdot 10^9) - 147.5 \text{ dB}$$

$$\underline{FSL(dB) \simeq 40.3 \text{ dB}}$$

The figure 3.6 on the following page shows the FSL as a function of frequency and radius as well as the specific losses for 900 MHz and 2.45 GHz.

3.3.5 Calculation

$$RxP = TxP + TxG - TxL - FSL - ML + RxG - RxL$$

$$Received power = 36 \text{ dBm} - 40.3 \text{ dB}$$

$$Received power = \text{-}4.3 \text{ dBm}$$

To convert dBm *t*o watt we use the formula:

$$\text{watt} = 1 \text{ mW} \cdot 10^{\frac{\text{dBm}}{10}}$$

Then we get:

$$1\text{mW} \cdot 10^{\frac{\text{-}4.3 \text{ dBm}}{10}} \simeq 0.35\text{mW} = 350\mu\text{W}$$

If a 50 Ω antenna is used:

$$P = V \cdot I = V \cdot \frac{V}{R} = \frac{V^2}{R} \Rightarrow$$

$$\text{V} = \sqrt{350 \cdot 10^{-6}\text{W} \cdot 50\Omega} = 0.135 = \underline{135 \text{ mV}}$$

This result will vary with antenna gain and environmental variables like humidity and reflections, but this estimate gives a good indication on how much energy the tag can receive from WLAN signals. Chapter 5 on page 41 describes how a CMOS charge pump can take advantage of this effect to create a supply voltage for a RFID tag.

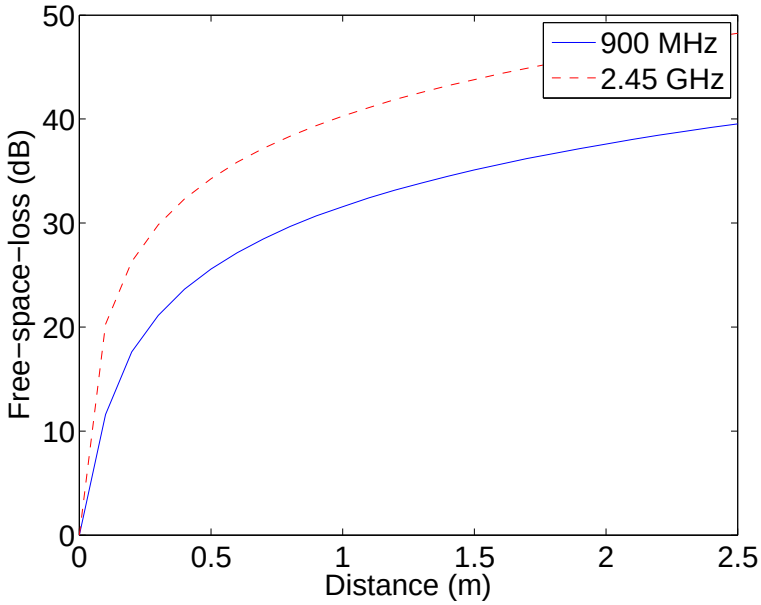

(a) FSL as a function of distance at 900 MHz and 2.45 GHz

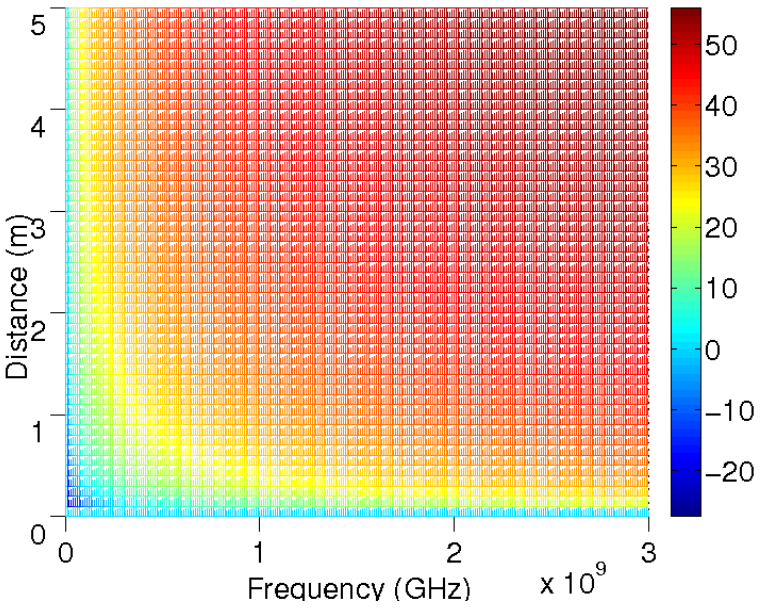

(b) FSL as a function of distance and frequency

Figure 3.6: Free space loss

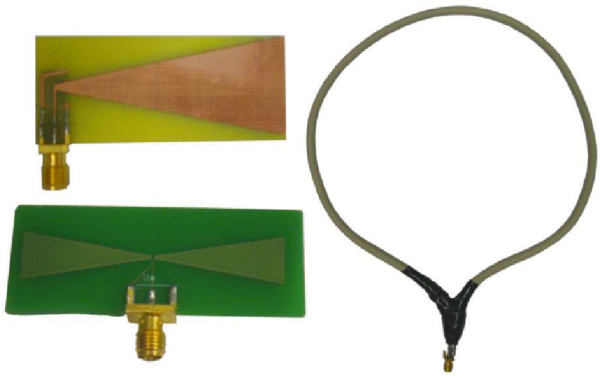

Figure 3.7: Antennas used in the measurements at 1 and 2.45 GHz

From literature on the subject (i.e. [Zhou 03]), we can read that wireless tags often receive up to 100 µW, and AC inputs of around 100 mV. To compare the theoretical estimate with the reality, a test with real antennas and transmissions was preformed. A signal generator with ability to generate high frequencies was used with an antenna to broadcast a signal with a certain amplitude and frequency. At the receiver antenna the signal was logged by an oscilloscope. Three different types of antennas where used; monopol bowtie, dipole bowtie and 25 cm loop antenna as shown in figure 3.7.

Various frequencies and energies where transmitted and measured at different ranges. When sending 1 V amplitude through the antenna at both 1 GHz and 2.45 GHz, up to 500 mV was received at the second antenna when the distance was a few centimeters. At longer ranges, up to 1 m, the received signal had a maximum of 100 mV. Altough this was not performed with antennas made exactly for these frequencies and this purpose, it shows that it is possible to receive signals in the hundreds of millivolt scale at these frequencies. It is not an easy task to use air as a conductor, as described in chapter 3.3.4, but still these signals are strong enough to make use of in a wireless scenario. To better understand what the purpose of the prospective power harvest is, we will now review some transmission methods commonly used in wireless communication.

Chapter 4

Transmission of data

To understand wireless communication technologies like RFID, we also have to understand the last step of the system, the transmission of the ID. The transmission of the data from the tag to the receiver is a crucial part of the system, because the power and space restrictions of the tag make the process quite complex. In addition to these requirements, the coding of the unique identification code of each tag is important to make the system work with several tags simultaneously. There are different ways to transmit signals from a chip, and some of the most common principles are described in this chapter, together with a comparison of these.

4.1 Analog modulation, AM and FM

The traditional way of transmitting a signal in a wireless manner is to modulate the signal on a carrier frequency. This is used in radio-communication since early 1900, and the signal is either modulated by amplitude (Amplitude Modulation (AM)) or frequency variations (Frequency Modulation (FM)). The first form of amplitude modulation was introduced in the mid-1870s under the name "undulatory currents", but not used in a practical way for radio communications before Reginald Fessenden demonstrated the AM transmission we know today early in the 1900's [Raby 70]. AM transmissions consist of a carrier with a certain frequency and a signal to be transmitted. Mixed together the resultant is a signal varying in amplitude according to the signal we want to transmit. This is an intuitive and easy implementation, but not very power effective. Much of the power is used in the carrier signal and this signal does not consist any information. An important consideration is the bandwidth, which here is the range of frequencies around the carrier frequency. As an example, an AM radio station has only 10kHz of bandwidth, with the carrier frequency in the center of the range. To use AM to transmit music is therefore not preferred as the musical range of the human ear is about 20

kHz, which is about twice the bandwidth of a standard AM transmission.

FM, on the other hand, is a bit younger method invented by Edwin Armstrong in 1935 [Arms 36]. In commercial radio broadcasting all over the world, frequency modulation is the standard way of transmitting signals. This is, as the name indicates, a modulation of the frequency rather than the amplitude, as in AM. The FM requires a wider bandwidth than amplitude modulation making it more suited for sound transmission. This larger bandwidth also makes the signal more robust regarding noise, interference and simple signal amplitude fading phenomena. The bandwidth of FM radio stations are around 200kHz, with the carrier frequency in the middle. The principles behind AM and FM are shown in figure 4.1.

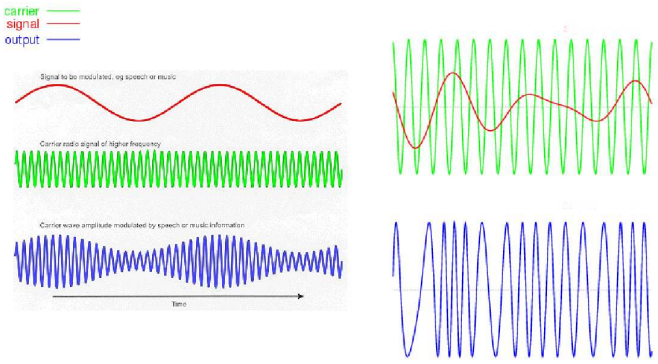

Figure 4.1: AM and FM modulation. (Courtesy of Wikipedia)

These modulation techniques described above are both analogue, hence both the transmitted signal and the carrier are analog signals. This is not preferable in passive RFID-tags because when generating an analog signal, an oscillator is needed. This can be implemented in active tags, but analog modulation of the signal is not commonly used. In most tags, digital modulation is the most common way to make a unique id.

4.2 Digital modulation, ASK and PSK

When the modulation of a signal is digital, the technique is basically an analog-to-digital conversion. An analog carrier signal is modulated by a digital bit stream. This bit-stream can be either of equal or varying length signals, and this modulation works much like an Analog to Digital Converter (ADC). The simplest form of digital modulation is Morse code, invented by Samuel F. B. Morse and Alfred Vail in the beginning in the 1830's [Mors 08]. This is a well known transmission method and consists of pauses, long and short pulses. This is much similar to the modern "bit",

and in many ways we can say that Morse-code is the predecessor to the digital bit. In modern RFID technology, digital modulation is the preferred way to transmit signals. Amplitude, frequency and phase shift keying is all used in RFID tags today, also in passive tags.

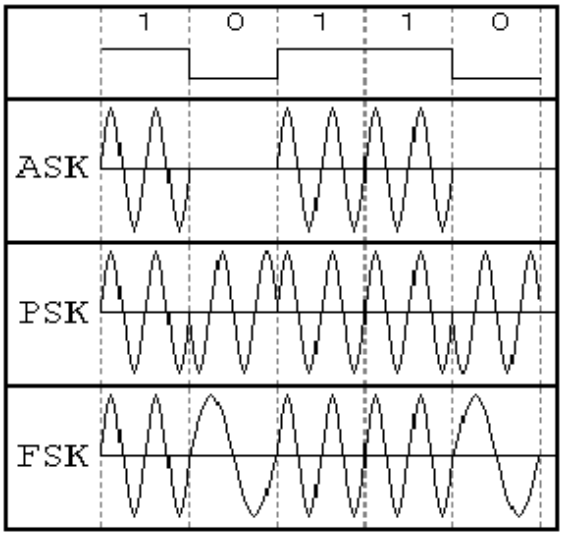

Figure 4.2: Digital modulation, ASK, PSK and FSK (Courtesy of Nakagawa Labs.)

ASK is the digital part of AM. A carrier signal is modulated by a bit-stream, keeping the frequency and phase constant. The different amplitude-levels is then representing 0's and 1's. An advantage with ASK is simplicity, and the modulation and demodulation is therefore quite inexpensive. The main drawbacks is that, in similarity with AM, ASK is a linear technique with high sensitivity to noise and distortions. To reduce the effect of the noise, the frequency can be modulated instead of the amplitude. This is called Frequency Shift Keying (FSK). With this method the signal shifts the output frequency between predetermined values. This was the common way to transfer signals in early telephone-line modems, which used the audio frequency-shift keying with rates up to about 300 bits per second. This is a modulation where digital data is represented in the frequency of an audio-tone, making is suitable for transmission via telephone or radio. The transmission has two states or tones, a mark which represent the binary one, and a space which represents the zero. This audio-modulated technique is not appropriate for high-speed communication, because it is not very efficient regarding power and bandwidth compared to other techniques. The advantages on the other hand, is simplicity and possibility to pass encoded signals through AC coupled links, including most equipment designed for music or speech.

The principles behind ASK, PSK and FSK are shown in figure 4.2 on the preceding page.

When designing a RFID system, it is important to choose the suitable transmission method. As we have seen, have all the techniques discussed above both advantages and drawbacks. A transmission technology demanding an on-chip oscillator will not be practical implementable in a passive wireless solution. This is because of the power required to run the oscillator will dominate, and the power demand of the tag will exceed the amount of air-born power available. Some of the transmission techniques can take advantage of the possibility to scatter the signal back, but this will also imply a more complex tag than necessary. To make this transmission power effective and simple, an impulse transmission also have to be considered.

4.3 UWB-IR

The conventional communication systems transmit information by varying the power, the frequency and/or the phase of a sinusoidal wave. Impulse Radio (IR) broadcasts by generating pulses where the information is modulated on the pulses by encoding the polarity, time spacing, amplitude, and/or by using orthogonal pulses [Bene 04]. Since the pulses are very short in time, they occupy a very large bandwidth, hence Ultra Wide Band (UWB). The transmission of pulses can either be sent sporadically at low pulse rates to support time/position modulation, or sent at rates up to the inverse of the UWB pulse bandwidth. The "FCC power spectral density emission limit" for the UWB band is -41.3 dBm/MHz. This is the same limit that applies for unintentional signals in the band, and therefore will the transmission strength be close to the noise in the band, see figure 4.3(a) on the next page. Since the strength is close to other unintentional signals and noise, this technique depends on repetition to succeed. Transmitting one unique train of pulses may not be recognizable, but repeating the sequence several times will make the sequence distinguishable from the noise. Because of this property, UWB-IR it is a viable candidate for short-range communications in dense multipath environments where the S/R-ratio (signal-to-noise) can be quite significant.

The properties of impulse radio transmission in the UWB band is, as we can see, suitable in order to transmit from an RFID tag with the specs given in this thesis. To transmit using impulse radio technology, an embedded pulse generator is required. A low-power pulse generator like this will not be discussed in this thesis, for further reading please see [Mars 03] or [Moen 06].

There are systems that do not use any complex pulse coding at all, and are truly passive. To review one example of this we will know take a closer

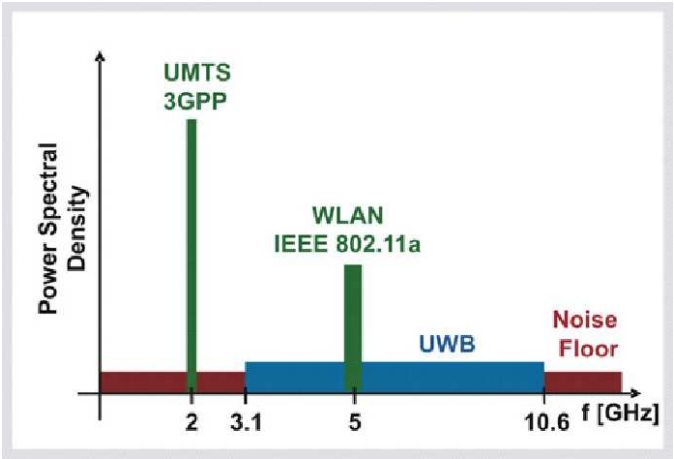

(a)

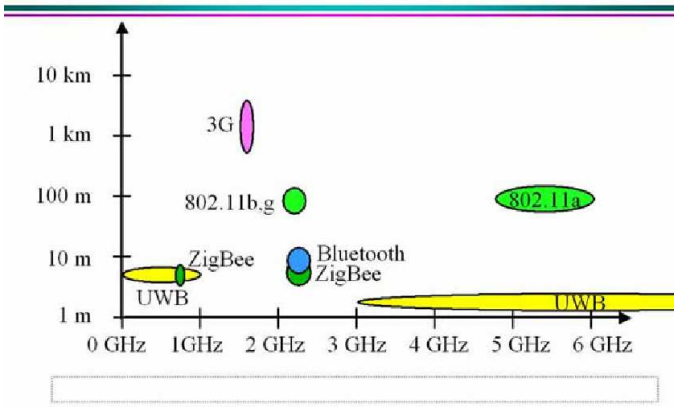

(b)

Figure 4.3: The UWB compared to other frequency bands (Courtesy of Institute for Integrated Signal Processing Systems)

look at SAW filters.

4.4 Surface Acoustic Wave filters (SAW filters)

Surface acoustic wave mode of propagation was first discovered by Lord Rayleigh, and the properties of these waves were reported in his paper from 1885 [Stru 85]. Lord Rayleigh, born John William Strutt, 3rd Baron Rayleigh, gave names to these waves, and today these are known as "Rayleigh waves". Rayleigh waves have both vertical and longitudinal components, which couples with the medium when they make contact with the surface of the device. This coupling affects the wave, and the amplitude and velocity will then change according to the characteristics of the material.

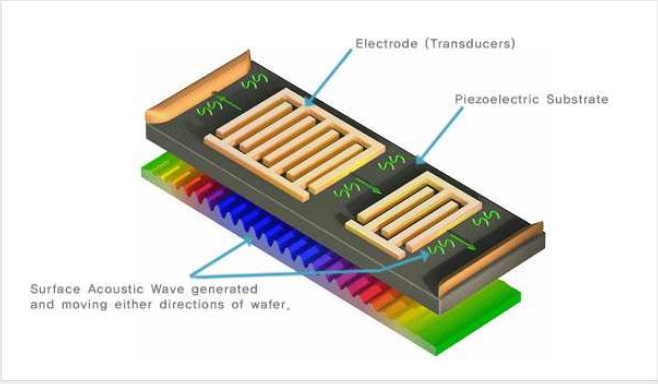

Figure 4.4: A Surface Acoustic Wave filter on a piezoelectric substrate. (ITF Co., Ltd.)

Lord Rayleigh, who got the Nobel Prize for Physics in 1904 due to his discovery of Argon, also discovered the foundation for SAW filters with his Rayleigh waves. These kind of filters are used in different identification systems, and was in the 1980's and 90's widely used in toll roads, i.e. in Oslo, Norway. The principles behind SAW filters are simple; the input signal is converted to a sound wave by a transducer, which creates a mechanical pressure in the material. This material, which is a piezoelectric material, then generates waves. These waves propagate along the surface of the material to a second transducer, which detects the frequency components of interest and convert these to electric current. The output of the filter is then "coded" with the characteristics of the material, and can be used to identify that specific tag.

The advantages with this kind of filter identification is that they have high tolerance to mechanical noise, temperature changes and movements, a high Q-factor and low production costs. Compared to silicon based RFID

is this a cheaper and simpler technology, but the SAW filter has some drawbacks. The filters have low efficiency, the output is quite damped compared to the input. This can of course be corrected with an amplifier, but amplifiers need a supply voltage, which again will make the RFID energy harvesting even harder. The SAW filters were replaced by semi-active silicon based RFID tags in the late 90's, because the semi-active silicon based tags had longer range and were more suitable for packing and sealing, making the tag more resistant to environmental strains.

No matter which kind of coding and transmission used, the tag still need energy. To power any type of tag with microwaves, RF energy or induction, an important part on the tag will be the energy harvesting. In the following chapters different energy sources will be discussed, as well as the different techniques of how to take advantage of them in order to transmit the tag's data.

Chapter 5

Voltage boosting

From the result of the link budget in chapter 3.3.3 on page 27, we can see that the calculated input voltage is far too low to power the tag. To generate a suitable supply voltage from the WLAN-signals, boosting and rectifying is needed. The typical supply voltage in a 90 nm process is around 1 V, and to achieve this the input voltage has to be multiplied by 10. On the other hand, a voltage below this value can be sufficient, but will depend on the system.

There are several ways to generate this supply voltage from the alternating input voltage, and some of these methods will now be discussed.

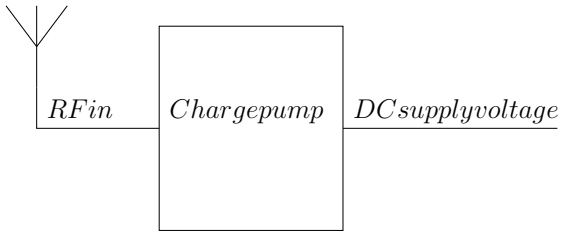

Figure 5.1: The input stage of a charge pump RFID-tag.

5.1 Boost and Buck converters

Boost and buck converters are technologies developed in the early 1960's when switches made from semiconductors become commercially available. One of the main motivations for this development was the aerospace industry that needed small, efficient and lightweight power converters in high numbers. Buck converters is used to scale down voltages and are not interesting under this topic. The boost converter technology on the other hand, is a type of circuit worth looking into.

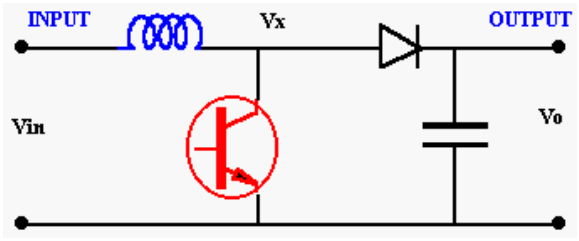

Figure 5.2: A conventional boost converter

The basic principle of a boost converter can be divided into two distinct states, the ON- and OFF-state, as shown in figure 5.3 on the next page. At the ON-state, the switch is closed and there will be an increasing current in the inductor. At the Off-state, the switch is open and the current from the inductor will have to flow through the diode and the capacitor C. After this state, the energy accumulated during the ON-state is transfered to the capacitor, resulting in a higher output than input voltage.

If we start by looking at blue path in figure 5.3 on the facing page, we can see that the switch is on(closed) and $V_x = V_{in}$. At the off-state the inductor current flows through the diode giving $V_x = V_o$. This is correct if we assume that the inductor current flows continuously and the diode is ideal. The average voltage across the inductor must be zero for the average current to remain in steady state.

$$V_{in} \cdot t_{on} + (V_{in} + V_o) \cdot t_{off} = 0$$

$$\frac{V_o}{V_{in}} = \frac{t_{on} + t_{off}}{t_{off}} = \frac{T}{t_{off}} = \frac{1}{1 - D}$$

where $T = t_{on} + toff$ and $D = \frac{t_{on}}{T}$ is defined as the duty ratio for the converter without losses. If the duty ratio, D, is between 0 and 1 will the output voltage be higher than the input voltage in magnitude, and this will always be the case for boost converters.

The boost converter can be useful for a RFID application, but if used, the input voltage to the tag have to be rectified because the boost converter is a DC to DC converter. To illustrate this, a boost converter just like the one in figure 5.2 is simulated for 2.5 ms with an inductor value of 500 µH, 200 mV DC input and a switch transistor with a pulse period of 50 µs. The circuit is simulated with 100 kΩ, 200 kΩ, 500 kΩ, 1 MΩ and 2 MΩ load. As we can see from figure 5.4 on the facing page, the volage boosting is considerably, at least with high resistance loads. This is because the output current will change in relation to the load and change the voltage according to Ohm's law; $U = R \cdot I$.

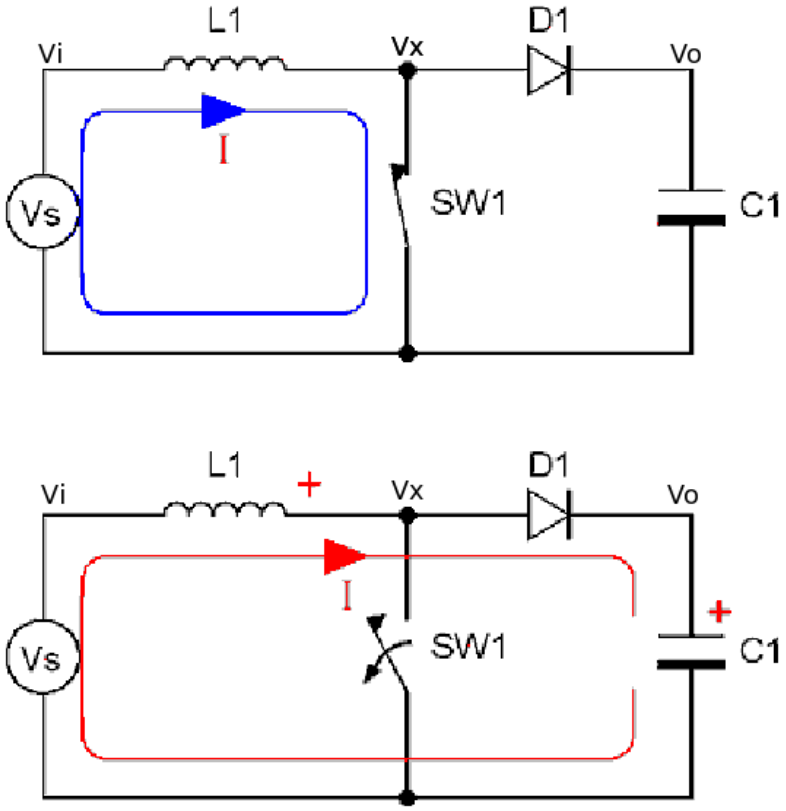

Figure 5.3: The states of a boost converter

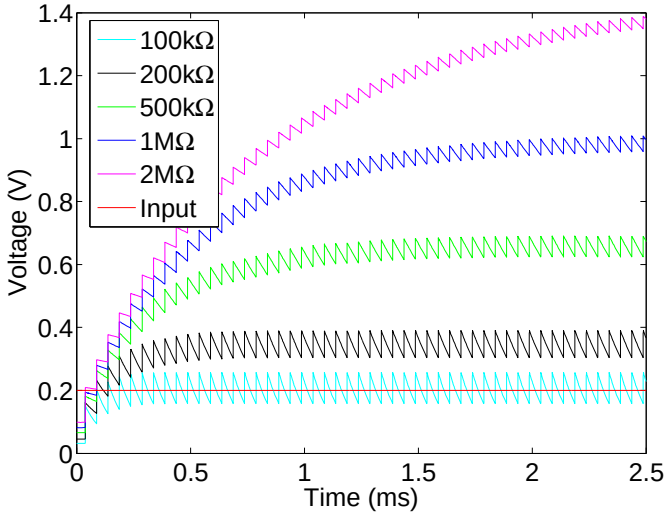

Figure 5.4: Input and output of a boost converter with different loads.

The use of boost converters with RFID is further discussed in chapter 5.7.

5.2 Charge pumps

Another method for raising a input voltage to a higher voltage level at the output, is by pumping charge by the use of a charge pump.

5.2.1 The Dickson charge pump

The charge pump technology is old, and one of the first and most basic version is the Dickson charge pump from 1976 [Dick 76], see figure 5.5. Most charge pumps use an AC input to generate a DC output voltage, and therefore also work as rectifiers.

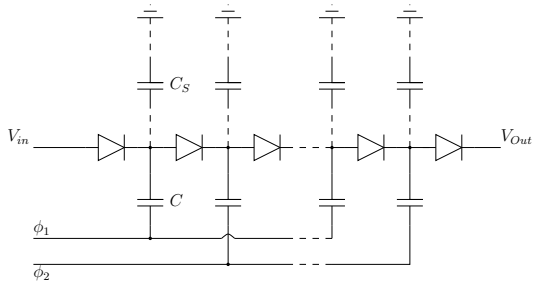

Figure 5.5: The mother of all charge pumps: The Dickson

This type of charge pump consists of two pumping clocks, ϕ_1 and ϕ_2, in opposite phase. The clock signals have a voltage V_ϕ, and the diodes work as switches. The Dickson operates by pumping the charge through the diodes, and charges the capacitors each clock cycle. Each step will add V_ϕ to the chain, but there will be a voltage drop at each diode, V_D. After N stages, a simple form of the output voltage can be written as:

$$V_{Out} = V_{in} + N \cdot (V_\phi - V_D) - V_D$$

There will be an extra V_D at the end of the equation because it is one more diode than steps in the pump.

The Dickson is a good choice for many applications, but in this case not optimal. Since an on-chip clock-generator requires both space and power, the Dickson charge pump is not a preferred solution for not only passive RFID tag, but for RFID generally. In a RFID case the input signal can be used as a shifting clocks, but is not preferred as the input signal typically is quite small and sometimes unstable. To avoid the need of clock-signals, a cascode charge pump is a far better alternative. This type of pump uses the

variations of the input signal to "pump" the charge through the circuit, and a rectified and increased voltage is produced. A number of cascode charge pumps are presented is various publications, but they are mainly variations of the same way of workings. The charge pump implementation in this thesis, see figure 5.6, is chosen because it is intuitive and produced good results even at small input signals. The motivation is from Udo Karthaus's paper about passive UHF RFID transponders [Kart 03]. The challenges with this circuit are to adapt the pump to a 90 nm CMOS process and make it more efficient at higher frequencies and with lower input voltages.

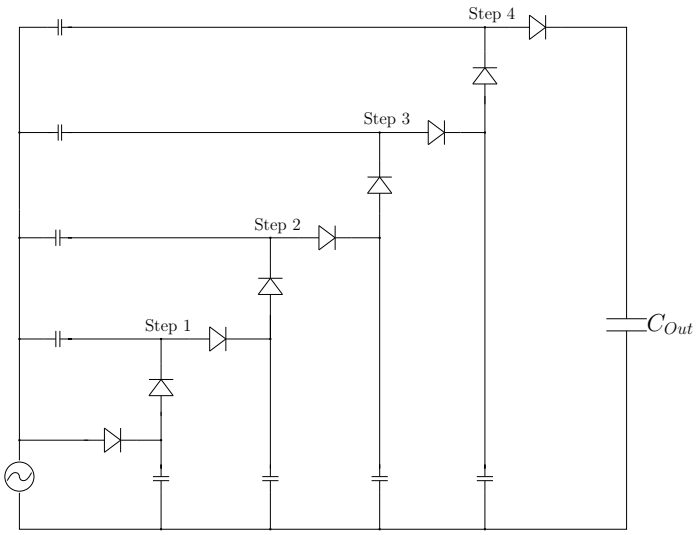

Figure 5.6: 4-step cascode charge pump

5.2.2 The cascode charge pump

The cascode charge pump in figure 5.6 is not very different from the Dickson charge pump, but has one huge advantage; not clock signal is needed. To find out how this is avoided we have to take a closer look at how the pump works.

The charge pump can be described as a series of steps. One of these steps is shown in figure 5.7 and the charge pump works as follows: The positive half period of the input will charge capacitor C_n and the diode coupled transistor will prevent the current flowing back. At the throughs of the input sine wave,

$$V_A = V_{n-1} - V_{th}.$$

At the peaks, this voltage rises $2 \cdot V_{in}$, and reaches

$$V_A = V_{n-1} - V_{th} + 2 \cdot V_{in}$$

C_n will be charged to $V_A - V_t$:

$$V_n = V_{n-1} + 2 \cdot V_{in} - 2 \cdot V_{th} \tag{5.1}$$

Each step of the charge pump can not increase the pumped voltage more than two times the amplitude of the input voltage minus two times the threshold voltage of the transistors. If the low-threshold models in the 90 nm technology are used, the diode threshold voltage will be 0.18 V. This means that, with no modifications to the circuit, the input amplitude must exceed 0.18 V to get the charge pump to pump voltage through the steps towards the last capacitor. With the backgate connection proposed later in this chapter, the charge pump can work at even lower inputs. We have to keep in mind that the equation above regards a charge pump with ideal diodes, and can be considered a good approximation. A more practical analysis will follow later in this chapter, in equation 5.2 on page 52.

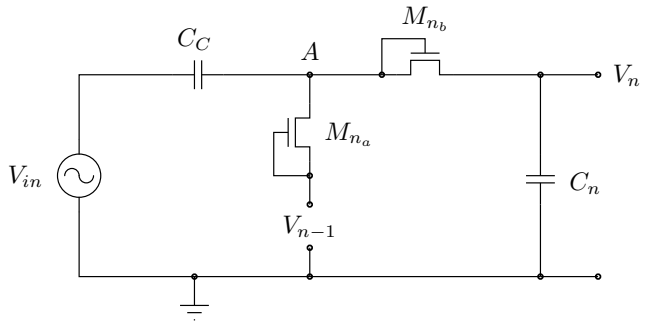

Figure 5.7: One step of the charge pump

To maximize the output voltage in this circuit, there are two main factors; minimize the threshold voltage or increase the number of steps. Since increasing the number of steps will cause degradation of power and conversion efficiency and also increased circuit size, lowering the voltage drop of the transistors is the most efficient way to improve the charge pump.

If we take a look at the threshold voltage of a transistor in the triode region [John 97], we can see the relationship between the transistor current and W/L.

$$I_{ds} = \beta \cdot \left((V_{GS} - V_t) \cdot V_{DS} - \frac{V_{DS}^2}{2} \right)$$

$$\beta = \mu_n \cdot C_{ox} \cdot \frac{W}{L}$$

To ensure pumping at low input voltages we will need a low V_{th}, and to ensure that we are able to deliver as much current as possible, W/L and

capacitors must be as large as possible without the capacitive load at the input of the circuit becoming too large. This can potentially be a problem in a practical implementation, because the input source will then not be able to drive the charge pump.

During this chapter the workings of the chosen charge pump have been described. As we have seen, are the diode coupled transistors an important part of this circuit and should be taken a closer look at. The threshold voltage of the transistors is important since the system is dealing with low voltages, and therefore will be further explored in the next chapter.

5.3 Adjusting threshold versus the leakage

The most important part of the charge pump is the diodes and the optimal rectifying element would be a device with low or no resistance when forward biased and with no conductance or infinite resistance when reverse biased. The normal diode forward biasing voltage of 0.7 V makes junction diodes unsuitable for power harvesting. Incoming antenna signals are normally $<$100 mV and the forward biasing voltage must be within the range of the received signal, and the substitute of a junction diode in CMOS is a diode-connect MOS transistor. In addition, a number of different threshold voltages are available as different devices (low threshold, standard threshold and high threshold). Also low leakage (low power) devices are provided, but sometimes the transconductance is reduced. As shown in figure 5.8(a) on the next page, the differences between the threshold voltages are significant when comparing the 3 different devices of 90 nm MOS transistors.

In figure 5.8(b) on the following page the PMOS and NMOS low threshold models are compared. Both with the same width and length. Width is here set to 100 µm and length to 0.1 µm to ensure that we are able to deliver as much current as possible, as explained in section 5.2.2 on page 45. As we can see the PMOS diode is by far the diode that leads the highest amount of current in the sub-threshold region. If the diodes are swept with a higher voltage, typically above 0.3 V, the NMOS diode will increase in a faster manner than the PMOS, but since the chargepump will have a input below that voltage, the PMOS is the preferred solution. This will be explained in the next section. Altdough the PMOS is the best of these models, it has the potential to be improved as we now will investigate.

5.4 Diode characteristics

In order to make the charge pump maximum efficient, the threshold voltage of the diodes have to be low when pumping the voltage, in order

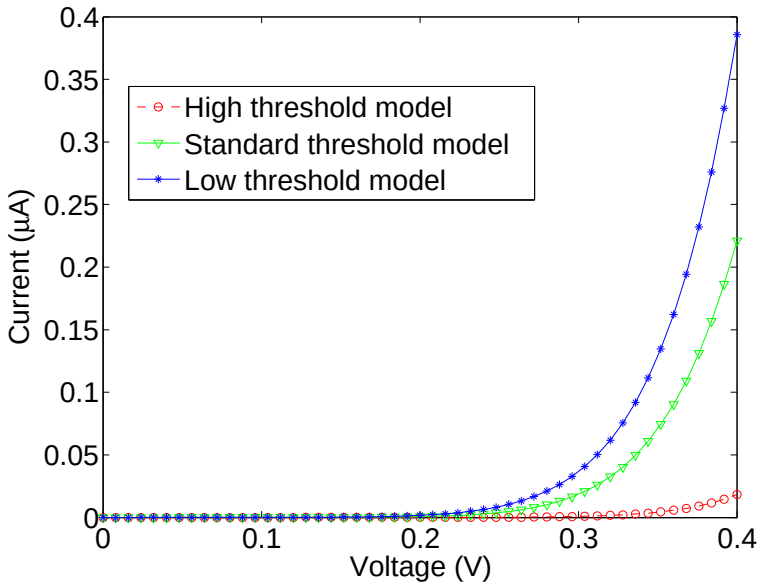

(a) Diode coupled MOS transistors. Simulated with minimum sizes.

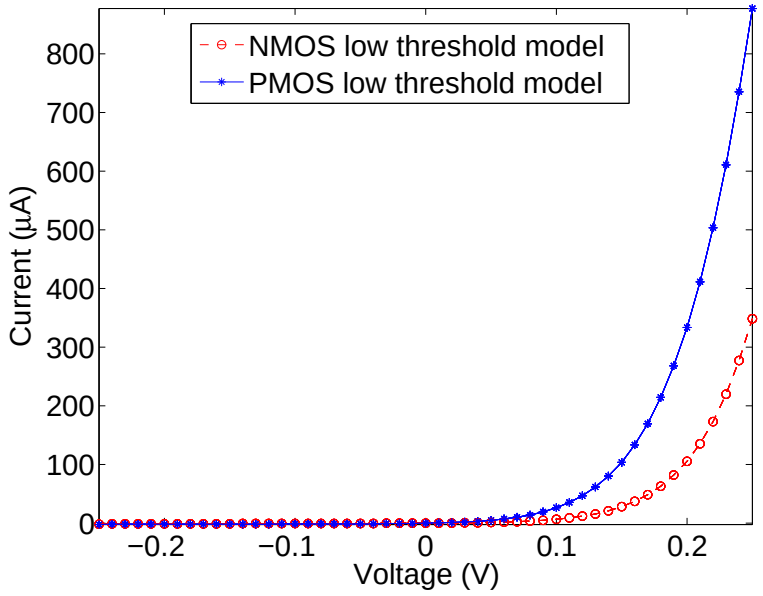

(b) Low threshold models of PMOS and NMOS.

Figure 5.8: Comparison of different MOS models

to get the voltage drop minimized. On the other hand when pushing the charge further on, at the negative half-period of the input, a high threshold is needed in order to reduce the leakage in the reverse direction of diode as much as possible. To adjust the charge pump to the better, we first need to understand the characteristics of the diodes.

When connecting a transistor as a diode, the idea is to create a channel below the gate when a certain difference in potential is applied to between drain and source. Since the channel is controlled by the gate, the gate is connected to one of the terminals. We often define this terminal as drain, since a higher potential is needed at the terminal connected with the gate to open the channel. If this potential becomes higher at the terminal not connected to the gate, the drain and source will be switched. (For NMOS). The forward channel current will then decrease and only the leakage current of the transistor is left, flowing in the reverse direction.

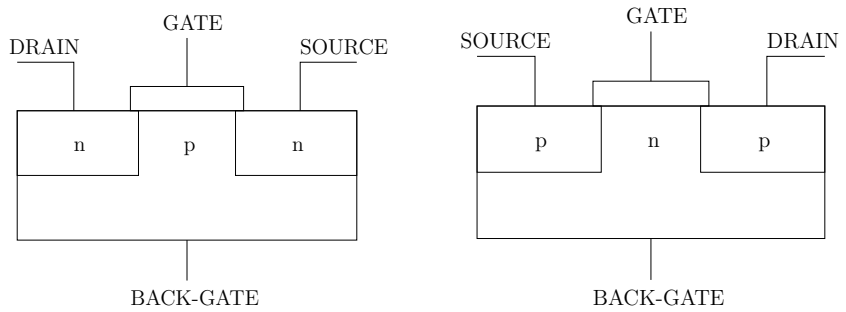

(a) NMOS (b) PMOS

Figure 5.9: The terminals of NMOS and PMOS transistors.

5.4.1 Adjusting the diodes

The secret to make an efficient pump is, as described above, to use diodes with both low threshold voltage and leakage voltage. This is a major challenge as these two factors are generally inverse proportional to each other. Some tweeking can be done, and in addition to low-threshold models, the back-gate can also be used to increase the pump effect.

The reason why the PMOS diode with bulk and gate connected together works as well as it does, is because of the "second" gate, and when connecting bulk to drain, the channel concentration of ions will be altered. The bulk connection, often called the back-gate, works in the same way as the gate, but it is not that effective. The sum of the two gates opening the channel will still cause a higher I_d at lower gates voltages. A gate voltage that is applied to both gates simultaneously. The reason the current through

the PMOS transistor is increasing at a lower voltage than the NMOS, is the level of doping and threshold voltage. The doping of the PMOS well is higher than the doping of the NMOS substrate, because of the increased mobility of the NMOS. This will lower the threshold, hence increase the current at lower voltages.

The threshold voltage can be expressed [John 97] like

$$V_{th} = V_{t_O} + \gamma \left(\sqrt{V_{sb} + |2\phi_F|} - \sqrt{|2\phi_F|} \right)$$

where γ is the body-effect parameter, $2\phi_F$ is the surface potential, and V_{th} is the zero bias threshold voltage.

As we can see from the equation above, the V_{sb} is a parameter that can be altered to achieve a low V_{th}. The back-gate connection can be described as a change in the bulk potential, hence causing a reversed body-effect. The body-effect is an effect describing changes in the threshold voltage of the transistor by the change in the source-bulk voltage, V_{sb}. Even these diodes will operate in a subthreshold area, the working way of the transistors will be the same. In subthreshold operation, this is even more important. To investigate this factor, the diode current is simulated as a function of voltage.

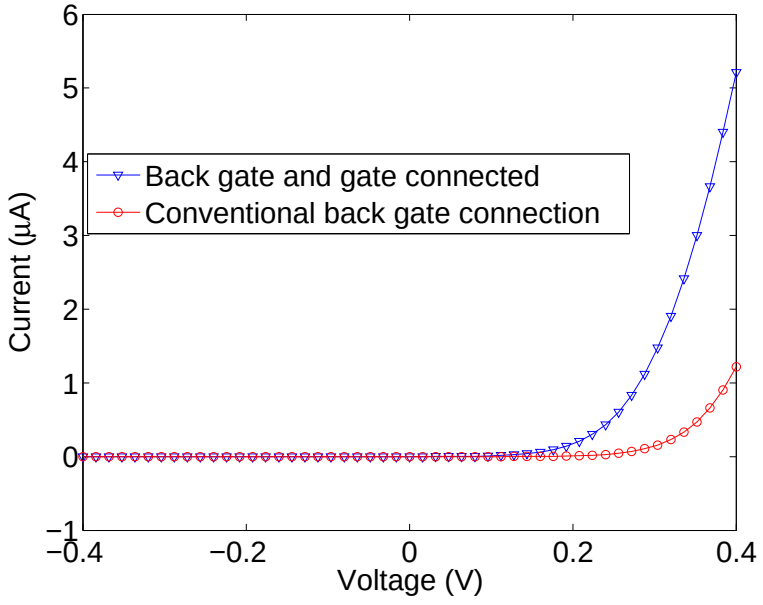

Figure 5.10: A diode connected PMOS transistor (low threshold model) compared to one with gate and backgate connected. Simulated with minimum sizes.

In the following simulations the test bench is swept with a voltage from

-0.4 V to 0.4 V, which will be more than sufficient range compared to the input AC of the actual circuit. During the sweep, the diode current is measured for different types of diodes and the prospective aberration is shown. The meaning of this study is to see which diode that has the best ratio between current at low voltages in forward direction and the leakage in the backward direction. It is important to choose a solution that has a higher exponential growth regarding current above, than below 0 V. This is important because this difference creates the pumping effect in the charge pump.

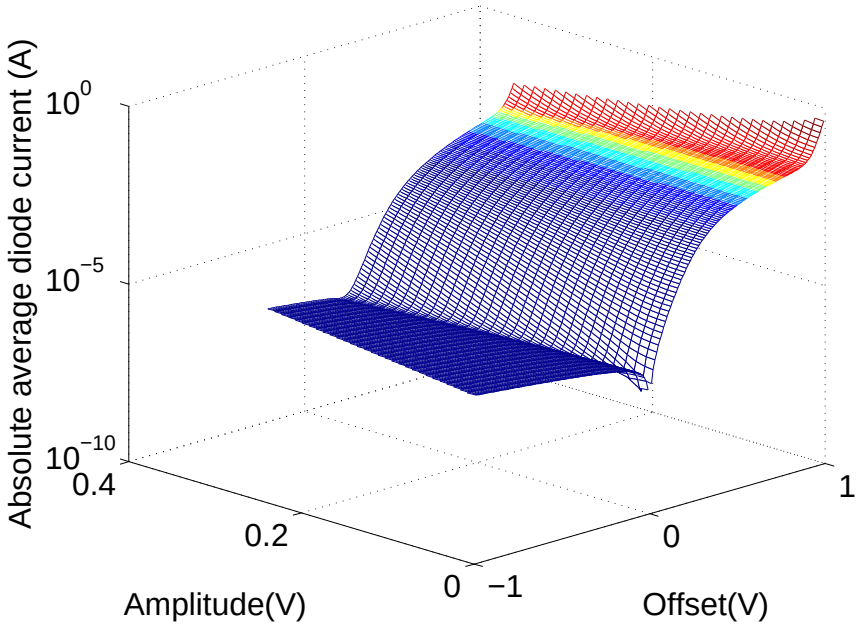

Figure 5.11: PMOS diode characteristics - The diode current as a function of offset and amplitude.

The diodes in the charge pump will be operating on a AC signal with amplitude of approximately 100 mV, but the signal will not always alternate around ground level. With time, each step will build an offset. This is because C_n will be charged until the forward diode current and the leakage is equal, when the average current through the diode is zero. In figure 5.11 the diode current is simulated as a function of offset and amplitude across the diode. Here, the diode current is interpolated with a generated sinusoidal with a given offset and amplitude. The offset is an important factor since it is the offset that will charge each step, together with the amplitude. This will give us important information regarding how the diodes will behave with time, and where the stabilization point of the diodes are.

The most important info from figure 5.11 on the page before is that the stabilization point of the diode, where the average current is zero, is below zero offset. This means that C_n can be charged with the difference from the stabilization point to zero offset. This can be seen even clearer on figure 5.12 on the facing page that shows the offset with fixed amplitudes for both low and standard threshold transistor models. Here we can see that the pump effect will increase considerable with higher amplitude. All this is because of the exponential growth of the diode current. It is the absolute value of the diode current that is shown in figure 5.12 on the next page. This means that the minimum, the dip, of each plot is the point where the current drops below zero, and switches direction. The reason why this minimum is not closer to the negative infinity, which will be zero on a log scale, is because of the resolution of the plotted data. Still, this minimum is easy to see, even at the 100 mV plots. Figure 5.12(e) shows that with a 100 mV input amplitude, the stabilization point of the diode will be around 75 mV. If we again look at 5.7 on page 46, we can now express the output voltage of each step as a function of the offset of each diode:

$$V_n = V_{n-1} + 2 \cdot V_{stabile} \tag{5.2}$$

where, V_{stable} is the stabilization of the offset in the two diodes.

Figure 5.12 also shows a soft-well PMOS transistor. This is a coupling that will increase the potential of the back-gate of the transistor, altering the body-effect. Not commonly used, but gave promising results, altdough not better than the PMOS with gate and back-gate connected. (It is hard to see the difference in figure 5.12, but the back-gate connected PMOS is slightly better than the soft-well PMOS.)

In the charge pump layout, presented later in this chapter, the pump are designed with PMOS diodes with back-gate connection as described in this chapter, and the high $\frac{W}{L}$ relationship. This is as we have seen, to ensure improved pump effect.

5.5 Capacitors

The choice of capacitors to use with the charge pump is important as these are responsible for storing the charge at each step of the pump, as well as DC block the input from the accumulated charge. One huge problem, litterally speaking, with capacitors in a CMOS process is the size. Large capacitors demands large area, and with limited space on a chip, embedded capacitors are a challenge.

The space available on the chip that will be sent to production, is 300 µm x 200 µm. To meet the requirements of size and value, various capacitors were simulated and tested in the circuit. A solution to the problem with large areas, is placing the capacitors off-chip and connect them via pins,

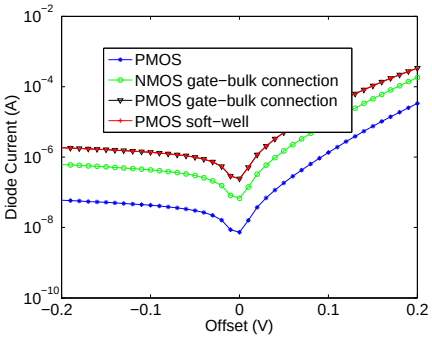

(a) 20 mV amplitude.

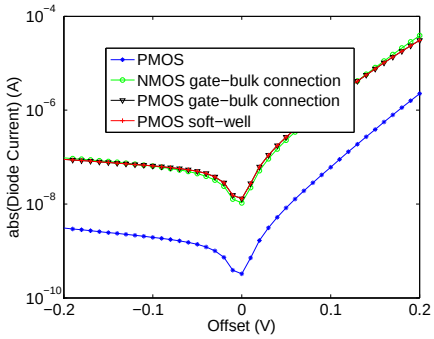

(b) 20 mV amplitude.

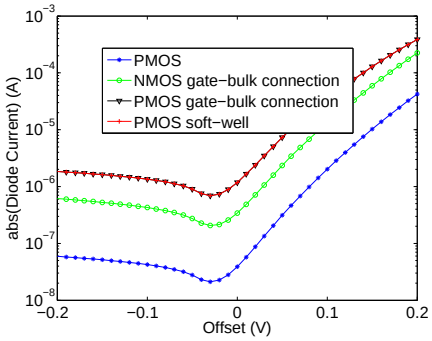

(c) 50 mV amplitude.

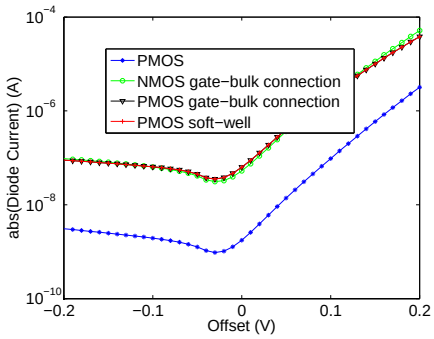

(d) 50 mV amplitude.

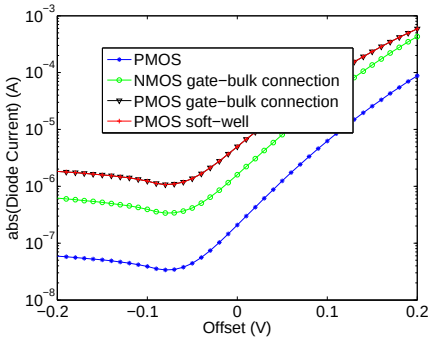

(e) 100 mV amplitude.

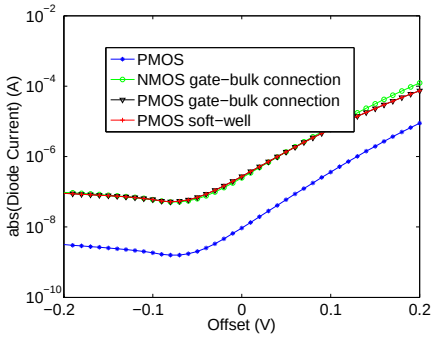

(f) 100 mV amplitude.

Figure 5.12: The diode current as a function of offset with fixed amplitudes. Low threshold models on the left, standard threshold models on the right.

Table 5.1: Capacitors in a STM 90nm CMOS process

Type	$\frac{\mathbf{fF}}{\mu m^2}$	**Description**
Fringe	1.2	Capacitor with "fingers"
MIM	2	Metal-Insulator-Metal
P-poly	5-15	Cap. between poly and p-well
pMOS	5-15	$C_{gs} + C_{gb} + C_{gd}$

but with this arrangement the inevitable capacitance of the pins will come into play, especially with RF signals In addition, it is the impractical part of having discrete components outside the chip. Some of the capacitors in the 90 nm design kit have large enough capacitance per area, but these are not linear with the voltage. Since off-chip capacitors are impractical and will affect the RF signal, the non-linear on-chip capacitors are the most optimal choice. As we can see from figure 5.14 on the next page, the output of the circuit is not that much affected by changes in the capacitor value, and nonlinearity will not be much of a problem even with the variation shown in figure 5.13.

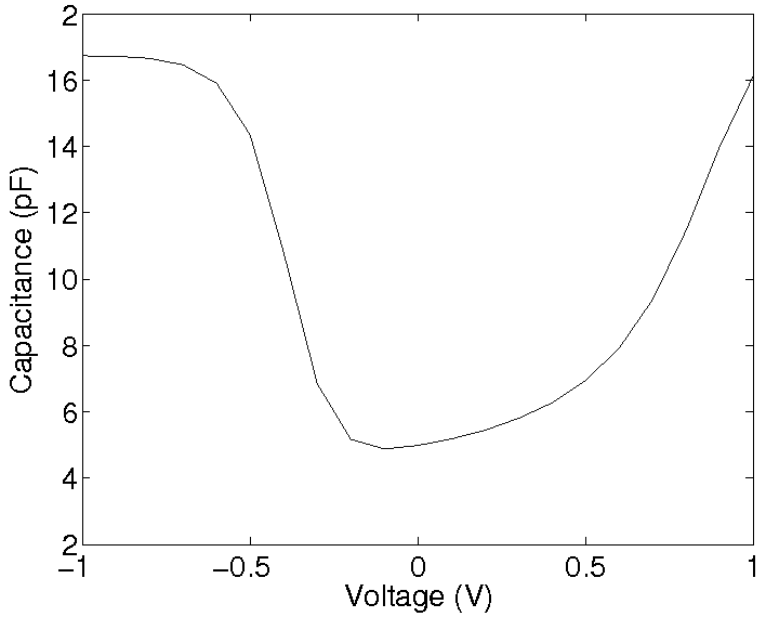

Figure 5.13: A CMOS transistor used as a capacitor is nonlinear regarding operating voltage.

The change of the charge pump output voltage due to capacitor variations is dependent of the time pumped. As figure 5.14 on the facing page shows, the smallest capacitance increases the most from time 0, but

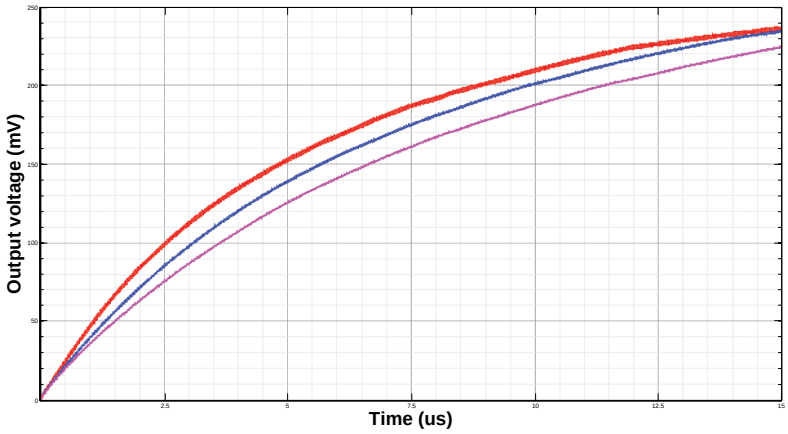

Figure 5.14: The charge pump output simulated with 5p (red), 10p (blue) and 15p (purple) capacitors.

the larger capacitors will have the ability to store a higher voltage over time.

5.6 Dual charge pump

The previous parts of this thesis have shown different ways to improve the pump. It has also been shown that even with this modifications, the pump is not adequate to power a RFID-tag with the given specifications regarding wireless power transfer. In chapter 5.2.2 on page 45, the charge pump described only exerts the positive half of the input. To take further advantage of the wireless power available, both the positive and negative swing should be taken advantage of. If this design is expanded to pump at both half, the result would be twice the output voltage [Curt 05]. This means that the voltage have to be, instead of pumped towards a output capacitance, pulled below the ground potential from an output capacitance. All the diodes will then have to be reversed to make the current flow from the output and produce this voltage drop. With the first implementation as a starting point, it is a simple task to implement this, as the expansion is just a reverse version of the pump that uses the positive half period. In figure 5.15 on the following page an implementation of this circuit is shown.

5.6.1 DC simulation

The simulation results show that this type of charge pump are significantly improved compared to the previous versions. If we define the ground

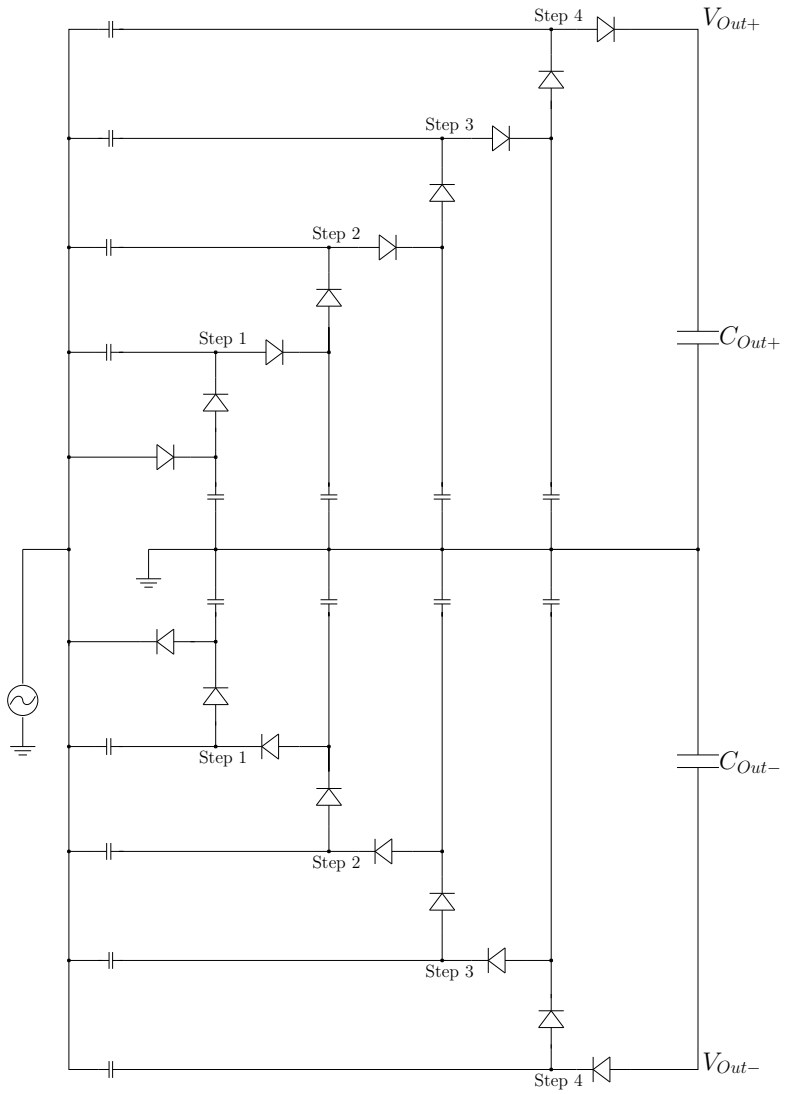

Figure 5.15: Charge pump that exploit both positive and negative half periods

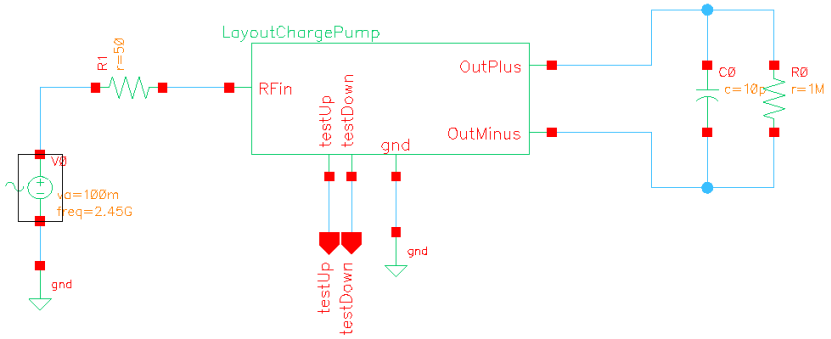

Figure 5.16: Testbench used to simulate the charge pump

potential as the negative output, a supply voltage up to 600 mV is available. This with just around 100 mV AC input swing to the charge pump. To make the circuit simulation more close to reality, a serial input resistance of 50 Ω is used to represent the resistance of the antenna. A output resistance of 1 MΩ at both at the positive and negative output is used in the simulations to represent a transmitter with high impedance attached to the charge pump, using the supply voltage generated. See figure 5.16.

As we can see from the results, is the performance of the circuit both dependent of the load and frequency. Frequencies in the gigahertz range generate a lower output voltage than in the megahertz range, due to capacitive losses. It is worth noticing that input signals with very low frequency will also result in a lower output voltage, since the input then is not alternating fast enough and the leakage in the transistors will deplete the charge between each cycle.

5.6.2 AC simulation

To find out how much of the RF signal that is left at the output of the charge pump, a AC simulation i performed. This is done by simulating the pump with a DC block capacitor at the output. As we can see in figure 5.18 on page 59, some of the AC input signal is left at the output, but this is below 5 mV and will not be a problem, since the DC is relative so much larger.

5.6.3 Process variations

To find out if the charge pump will be significantly affected by variations in the manufacturing process, the circuit is simulated with a Monte Carlo simulation. This will simulate the charge pump running several times, but with different sizes and values of the components. These changes represent the variations that can occur from one process to another or within the

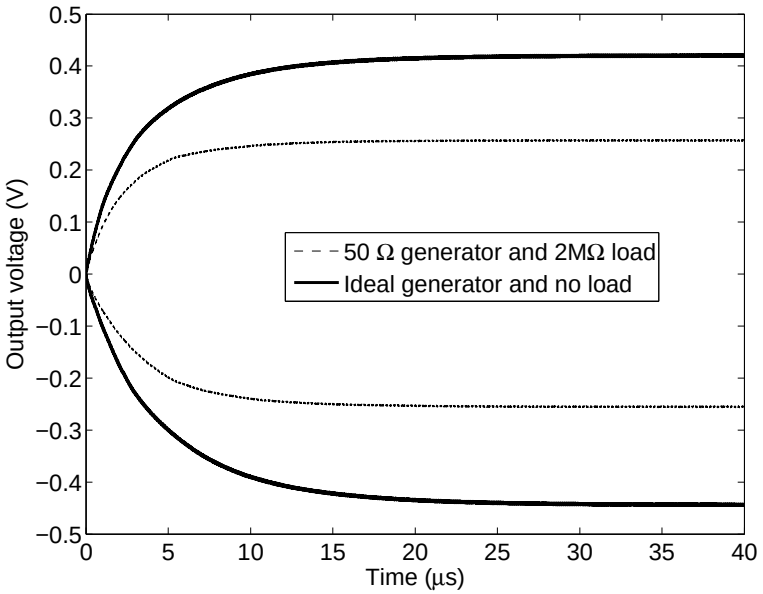

(a) 900 MHz

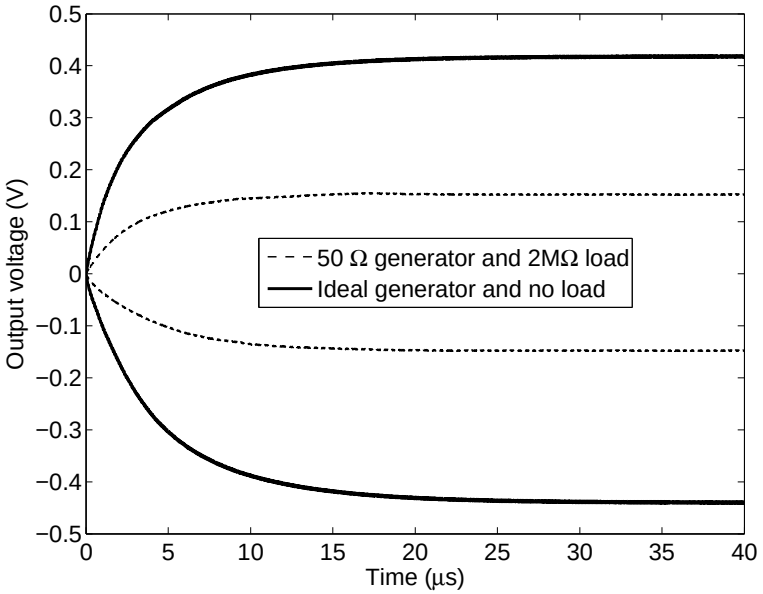

(b) 2.45 GHz

Figure 5.17: Time development of charge pump output

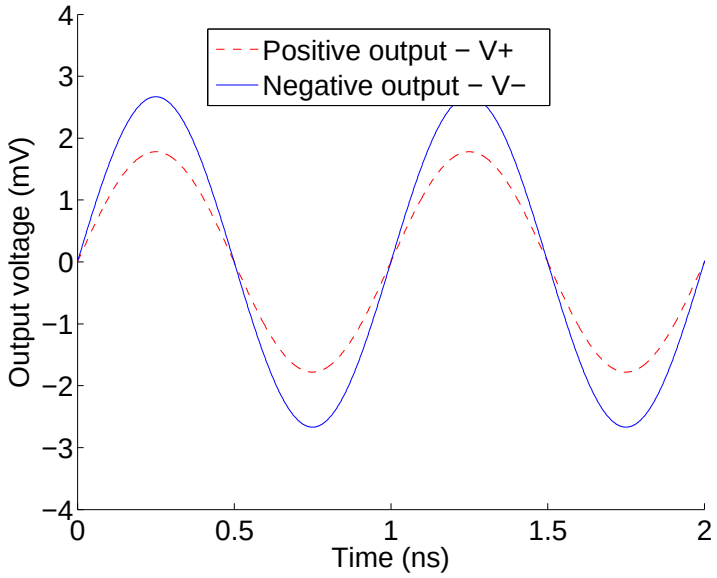

(a) 900 MHz

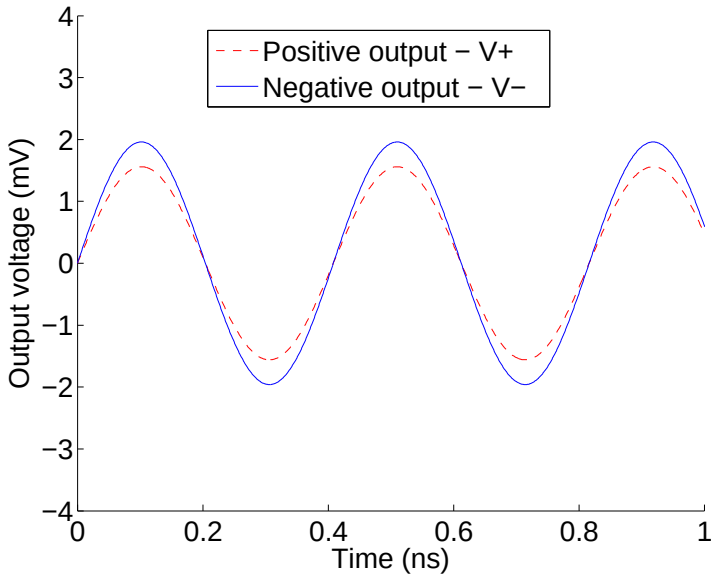

(b) 2.45 GHz

Figure 5.18: The AC component of the output voltage

same process. As we can see from figure 5.19, the variation in the output

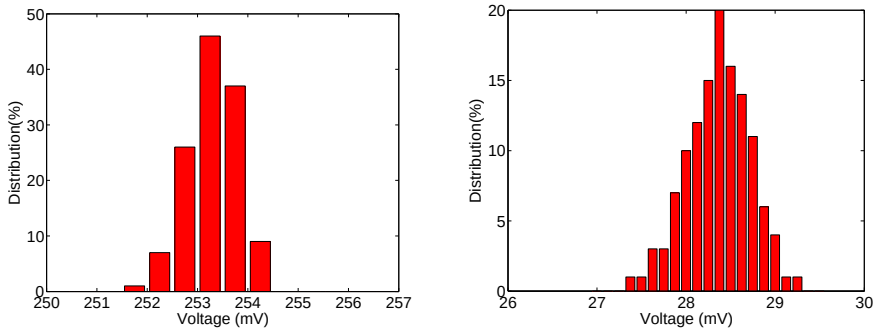

(a) Schematic (b) Layout

Figure 5.19: The changes in the circuit due to process variations.

due to the process variations is quite small. The standard deviation is well below 1 mV, when the output is about 250 mV. The circuits should behave in almost an identical manner, even from one "extreme" to another. The number of runs should ideally been higher, but this was not possible due to time and storage restrictions at the workstation where the simulation was preformed. The layout of the charge pump is simulated just a tenth of the time the schematic is, due to the same restrictions. Results of the Monte Carlo simulation are shown i table 5.2, where μ is the arithmetic mean, σ is the standard deviation and $\mathcal{N}$ is the number of runs.

Table 5.2: Monte Carlo simulation

	Schematic	**Layout**
μ	253.30 mV	28.35 mV
σ	521.49 µV	359.28 µV
$\mathcal{N}$	125	125

5.6.4 Layout of the charge pump

In figure A.1 on page 93, the layout of the the circuit is shown. The input capacitors are the large blocks on the left side, and the blocks on the right side are the capacitors connected to ground. The layout is arranged this way to separate the RF input on the left from ground, and this way minimize the capacitance directly from input to ground. Between these capacitor blocks, the transistors are placed, with the first steps of the pump in the center. The positive and negative output of the pump are placed top center and bottom center respectively, and ground is connected at the

right side of the circuit. The size of the layout is 260 µm x 160 µm, and also include outputs within the pump for measuring purposes during testing. Measurements of the chip are shown in chapter 6 on page 63.

5.7 Boostconverting of the charge pump output

The charge pump generates a DC voltage available for use. To use this voltage for transmitting pulses, the idea is to push all the charge out in a train of pulses, hence the charge should be as large as possible. When using the charge pump, the signals offset will be raised and the signal rectified. To further enlarge this voltage, a boostconverter can be used. As described in chapter 5.1, the converter needs a pulse alternating between safe below and above the threshold of the transistor switching the inner loop on and off. If a pulse like this is present, a boost converter will boost the voltage significantly. How large, will depend on the coil and duration of the convertion. The idea is shown in figure 5.20, but instead of a pulse generator, the pulse can be generated somewhere in the pump. This could not be successfully done with the charge pump described in this chapter, but can be done with other designs that have signals that oscillate enough to be able to control the switch in the boost converter.

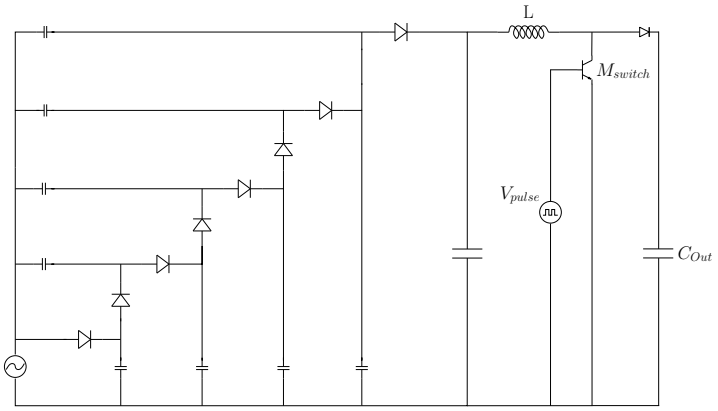

Figure 5.20: Boosting of the output with a pulse generator

Chapter 6

PCB, chip and measurements

The layout of the charge pump from chapter 5.6.1 on page 55 was sent to manufacturing at ST microelectronics in October 2007, and the chip arrived late Mars 2008. In the meanwhile a PCB was designed to fit the specifications of the chip and manufactured at Elprint. The schematic and layout of the PCB are shown in appendix B on page 95, and the specifications of the PCB can be found in table 6.1 on the next page.

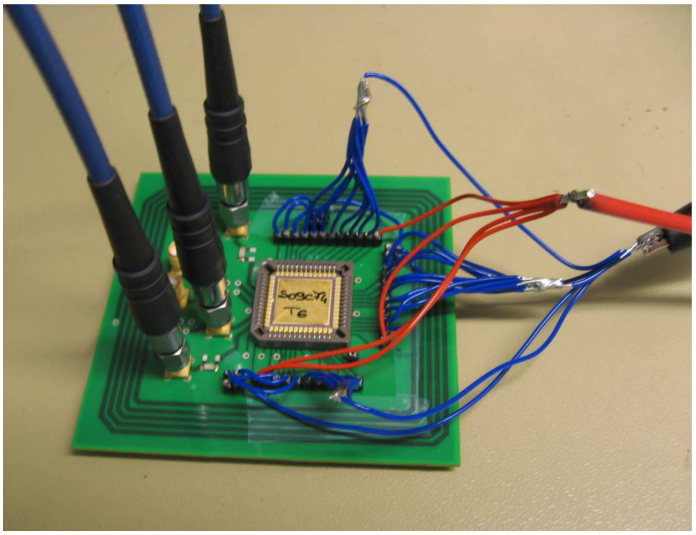

Figure 6.1: Test setup - PCB with chip.

The PCB is designed with connectors to all pins of the chip and SMA connectors to the charge pump in- and outputs. The chip is connected to the board with a surface mounted J-Leaded Chip Carrier (JLCC) with 52 pins, the same number as the chip. All pins which are not used by the charge pump, except for pad frame supply voltage pins, are connected to ground during testing. The RF conductor lanes are matched in size according to

50 Ω, to extend the transmission lines from the signal source to the chip.

Table 6.1: Specifications of Elprint PCB used.

Quantity	Material	Type	Thickness (mm)
1	copper plating		0.025
1	copper foil	18 µm	0.018
2	prepreg	7628	0.406
1	inner layers	18/18 Panasonic R1755	0.735
2	prepreg	7628	0.406
1	copper foil	18 µm	0.018
1	copper plating		0.025
		Total thickness:	**1.633**

Figure 6.1 on the preceding page shows the test setup, with SMA cables connected to the RF input, the positive and negative output. Ground and pad frame supply voltage are connected at the right side of the board. The outputs are simulated at 1 GHz and 2.45 GHz. This is because the high frequency signal generator used had a lower limit at 1 GHz. If 900 MHz is the desired frequency, the results will be very close to the measurements with 1 GHz.

6.1 AC measurements

The first measurement performed was a measurement of the AC component of the outputs. This measurement gives us information about how much of the RF input that is left at the outputs, V_+ and V_-. To find out how fast the AC is decreasing in strength through the charge pump, the AC component is also measured halfway in the pump, after two steps. The measurements are done at 1 GHz with an input amplitude of 100 mV, and are shown in figure 6.3 on the next page and 6.4 on the facing page. The test setup is shown in figure 6.2.

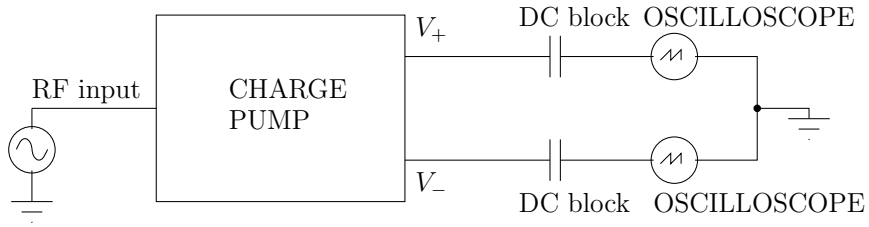

Figure 6.2: Test setup used to measure the AC component of the outputs.

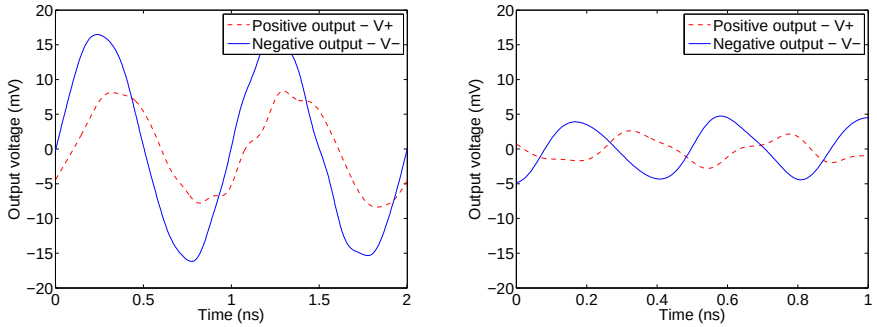

(a) 1 GHz (b) 2.45 GHz

Figure 6.3: AC component.

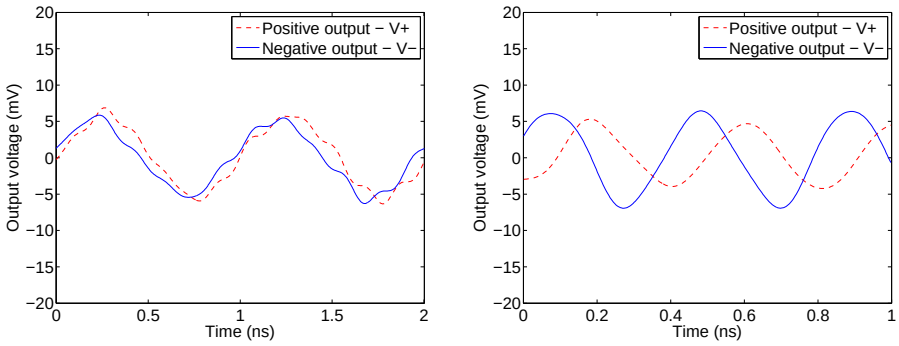

(a) 1 GHz (b) 2.45 GHz

Figure 6.4: AC component Test point.

6.2 DC measurements

To measure the output voltage of the circuit, with and without load, the test setup in figure 6.5 was used. The circuit was measured with input amplitude of 50 mV, 75 mV, 100 mV, 125 mV and 150 mV, and frequencies of 1 GHz and 2.45 GHz. The results are shown in figure 6.6 on the next page. The level of output voltage are plotted as a function of different input amplitudes. The default value of all the simulations was a input amplitude of 100 mV, since this was the maximum input one can expect from an antenna. These results are specified in numbers and are shown in table 6.2, and in the same table are the measurements from the test outputs halfway through the pump shown. The test setup is shown in figure 6.5.

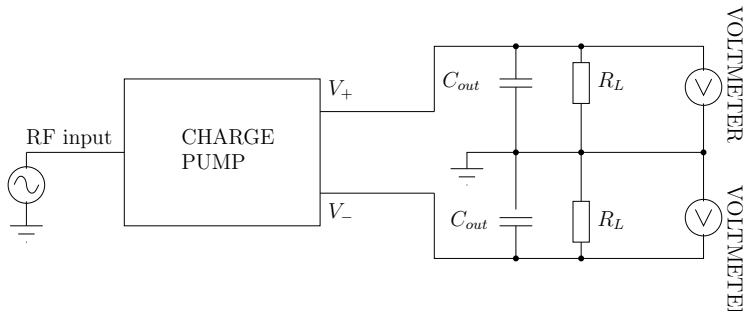

Figure 6.5: Test setup used to measure the DC output voltage.

Table 6.2: Measured output of the charge pump - Input signal with 100 mV amplitude

	No load		**1 MΩ load**	
	V_+	V_-	V_+	V_-
1 GHz	230 mV	-234 mV	240 mV	-240 mV
2.45 GHz	49 mV	-51 mV	54 mV	-56 mV

(a) Halfway through the pump, after two steps

	No load		**1 MΩ load**	
	V_+	V_-	V_+	V_-
1 GHz	440 mV	-454 mV	468 mV	-468 mV
2.45 GHz	85 mV	-91 mV	96 mV	-101 mV

(b) At the final output, after all four steps

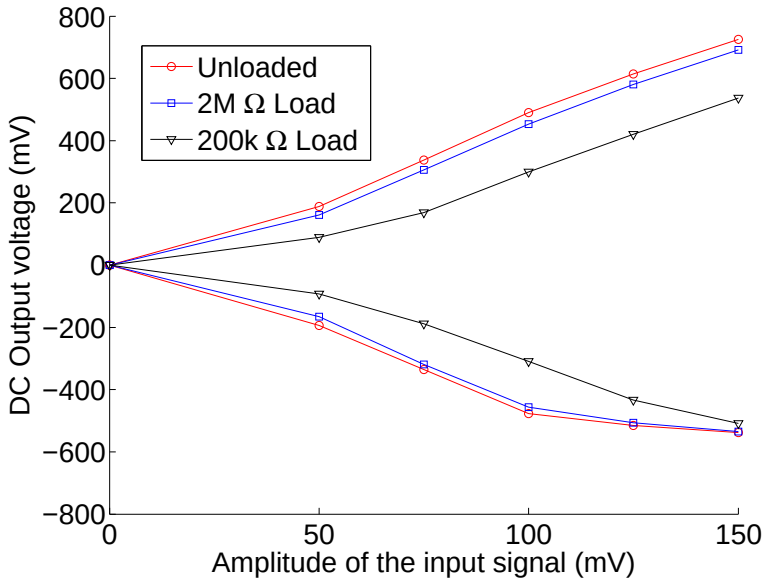

(a) 1 GHz

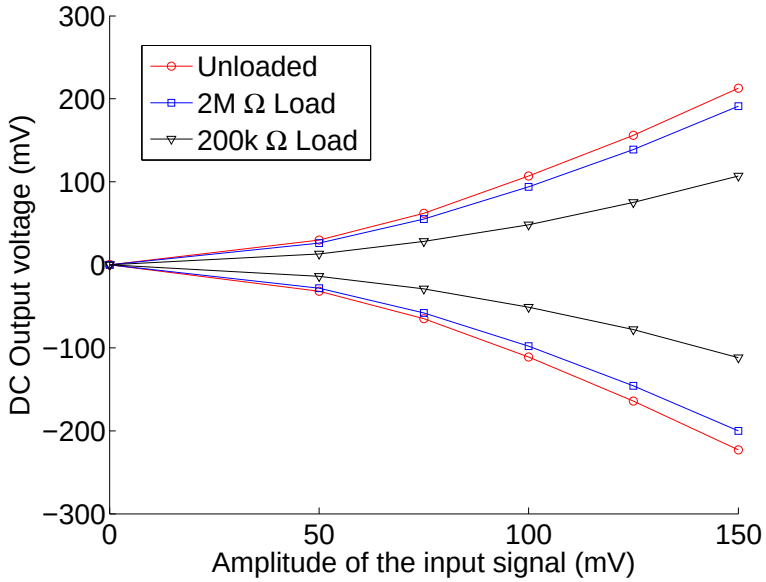

(b) 2.45 GHz

Figure 6.6: Output of the charge pump as a function of input amplitude.

6.3 Power measurements

To use the charge pump in a practical system, an important measure is how much power the circuit can deliver. In wireless communication tags the circuits are low power, but an embedded voltage supply should deliver power in micro watts scale, and sometimes as high as 100 µW. The power the charge pump is able to deliver was measured and is shown in figure 6.7 on the facing page. Here w can see how large input the charge pump will need to deliver a certain amount of power at different fixed output voltages. In figure 6.7(b) on the next page, the output current as a function of input amplitude with fixed output voltage is plotted.

6.4 Process variations

In chapter 5.6.3 on page 57, the process variations where simulated, and the result told us that this would probably not be a problem with this circuit. To get an idea of this, all 10 chips where tested during the same conditions and measurements and compared. From the best to the worst results, the difference in output voltage was 2.6 %.

6.5 Antenna measurements

The last measurement performed, was a test of the antenna on the PCB. The antenna, with diameter of approximately 70 mm is designed for a gigahertz transmission, and is connected to the input of the charge pump. To prevent unnecessary input load during the other measurements, the antenna is detachable and was only attached during this specific measurement. An 1 GHz signal was generated by a high frequency signal generator and sent to a loop antenna, and at the same time the DC output of the charge pump was measured. At long range, above 0.5 m, no significant signal could be detected, but at 0.15 m and below, the output of the pump showed DC voltages up to 200 mV. When there was no relative movement between the antenna and the PCB, the output voltage was fairly stable, with an oscillation below 10 mV.

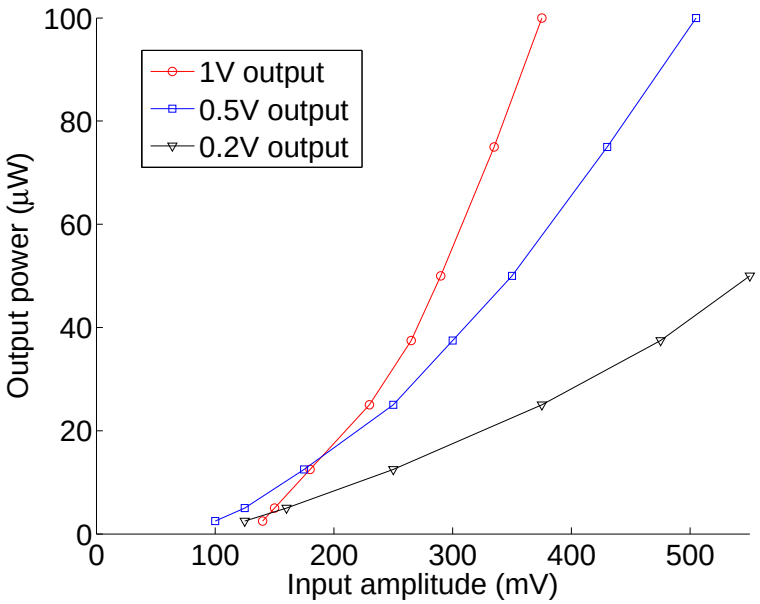

(a) Output power with fixed output voltage.

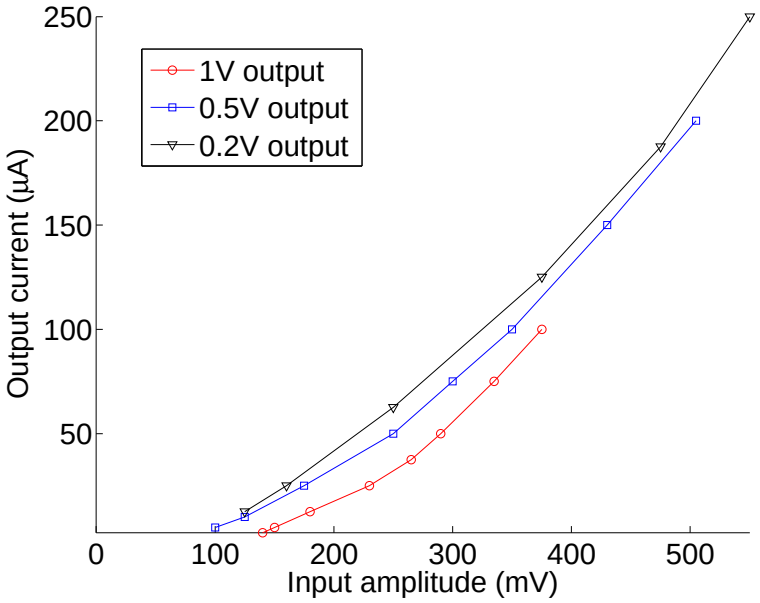

(b) Output current with fixed output voltage.

Figure 6.7: Output of the charge pump as a function of input amplitude.

6.6 Reflection of the RF signals

In figure 6.8 is the magnitude and phase of the reflection of the input terminal shown, also known as "S11" in a multiport RF reflection scheme. As we can see in figure 6.8, the reflected power ratio of 1 GHz is 11.85% and at 2.45 GHz this ratio is 42.34%.

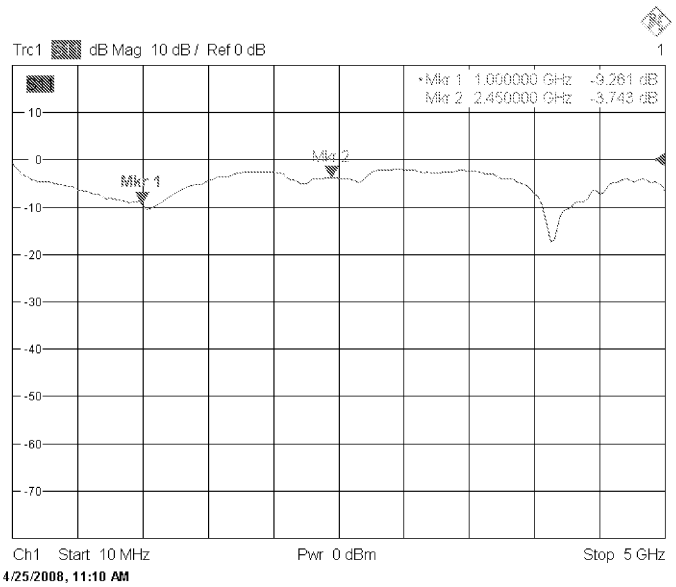

Figure 6.8: The reflection of the input terminal, S11, in terms of magnitude.

6.7 Discussion of the measurement results

The measurements presented in this chapter, gives a good insight of how the chip works. If these results are compared with the simulation results in chapter 5, we can see that the DC output of the chip is satisfying and a good match with the simulations. Figure 5.12(e) on page 53 states that at 100 mV input amplitude, the stabilization point of the diodes will be around 75 mV. If this is combined with equation 5.2 on page 52, we will get a theoretical output of the four step pump of 600 mV. This is close to what is measured. The simulation of the charge pump without load is quite similar to the measurements without load, but the results of the loaded charge pump is actually better in real life than in the simulations. This can be due to reflections, that will be discussed later in this chapter.

As we can see in figure 6.6(a), the symmetry in broken when $V_{\_}$ is below approximately -0.5 V. This is because the pad frame of the chip has diodes between the pads and ground to prevent overloading of the chip. They

have a reverse current threshold of around -0.6 V and limit the negative output at this level. This was not thought of as a problem when the pad frame was chosen, but have to be kept in mind if the design becomes a part of a commercial system.

The measurements of the AC component of the output in figure 6.3 on page 65 differs somewhat from the simulations at 1 GHz in figure 5.18 on page 59. This slightly increased AC component is probably a result of the padframe limitation described in the last section. The diodes appears as a load when switched on, and this constant "leak" will deplete C_{out} between the cycles. This will cause more variations at the output, as C_{out} has to recharge more between each input amplitude. Still the remains of the RF input at the output voltage is well below 20 mV. This will not be dominant in a system where the power is generated from more or less unstable electromagnetic waves. As we can see in both the simulation and the measurement, the positive output, V_+, has a smaller AC component, than the negative V_-. It is hard to say exactly what causes this difference, but it is probably due to the pad frame limitation of the negative output described above.

As we can see in figure 6.4 on page 65 the oscillation of the outputs after two steps have approximately half the amplitude of the oscillation of the final output at 1 GHz. This indicates that the AC components attenuates linearly, which correlates good with the simulations and the theory. At 2.45 GHz the AC part of the input signal will attenuate at an earlier stage due to the higher frequency. When looking at the phase of the output signal generated from the 2.45 GHz input, we can see that it is differently displaced at the positive than at the negative output. This is because the pump can be considered as a lowpass filter, with its capacitors to ground and diode resistance. Since the positive and negative outputs are generated from different "filters", the time constant, τ, are somewhat different and causing a different phase shift. The phase shift will not have any effect on the pump since we are only interested in the DC part of the output.

The amount of power the circuit should be able to deliver, depends of course on the device or circuit the pump is powering. Modern systems designed for wireless technology are in the category "low power circuits", hence they demand power in the microwatt scale. As figure 6.7(a) on page 69 shows, the power available at 100 mV input amplitude, is around 5 µW, which can be adequate to power certain circuit elements, but perhaps to low for a transmitter. As a comparison a modern low power flip-flop demands only a few nanowatts to operate [Alst 08].

Even small differences from a circuit to another is not crucial in this type of system, process variation should always be as low as possible. The simulations in chapter 5.6.3 on page 57 told us that process variation was quite small in this design, just hundreds of microvolts. Although it is not possible to get a statistical significant amount of measurements with

only 10 chips, these chips where put to the test. The difference of 2.6% from best to worse is acceptable and a few millivolts difference will not be significant as a supply voltage generated by airborn energy will never be dead stable. The chip used for measurements in this thesis is the one closest to the average regarding performance. There are always ways to improve the design in order to avoid mismatch and process variations, but nothing implies that it is a problem in this case.

When working with RF signals impedance matching is an important issue, and the reflections of the input terminal is probably the most considerable problem with this design. A reflection power ratio of 11.85% at 1 GHz means that 11.85% of the power introduced to the circuit is reflected back to source at this frequency. This phase shifted and attenuated version of the input is reflected back and can also cause interference with the incoming input signal. At 2.45 GHz, this ratio of 42.34% is more considerable. This means that the input signal at this frequency can affect the input with variations of $\pm$ 42.34%. The amount of variation depends on the phase in each point of the transmission line, and which again will depend on cable lengths, connectors and the source.

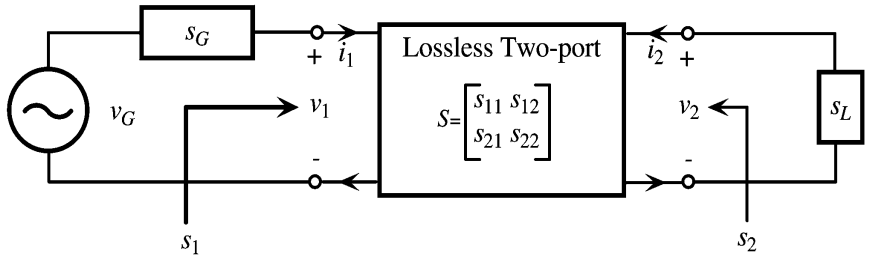

Figure 6.9: Lossless two-port with scattering matrix S connecting a generator with reflectance S_G to a load with reflectance S_L.

It is close to impossible to design a system with zero reflection at high frequencies, but a impedance matching network at the input can limit the reflection and maximize the power transfer significantly. This type of network consists of transformers, resistors, inductors and capacitors, and with the right values the output impedance of the source will be equal to the input impedance of the circuit [Ludw 00]. In this case, where we are interested in a power transfer and not just a single frequency, a wide band impedance matching will suit the design. This is not as trivial as a narrow band matching network, but narrow band matching will not prevent reflections at a multiple frequencies i.e. at 1 GHz and 2.45 GHz [Fano 48]. A matching network can be implemented on-chip or mounted on the PCB, either as components or bought as a complete IC solution.

Chapter 7

Alternative energy harvesting

The energy available from the circuits in the last section, may need to be combined with other ways of energy harvesting, dependent of the system using it. The selection of power sources to choose from is large, but is narrowed down to just a few candidates when the demand is that the technology have to be manufactured in a CMOS process.

7.1 Solar energy

Solar energy is a powerful type of energy more and more used in various contexts world wide. The main problem with solar energy has been that the technology was not mature enough for challenging other and more well-prooven technologies in real life applications. Now that the efficiency has been improved and the price reduced, this renewable energy source is being more and more popular, especially as energy plants in sunny parts of the world.

7.1.1 p-n junctions, photovoltaic cells and photodiodes

The cells in solar panels are made from semiconductors with high purity, almost without exception silicon. Semiconductors, as silicon (SI), have an energy gap between the conductor shell and the valence shell and conduct electricity quite poorly. To increase the conductivity the semiconductor, materials are doped with either a donor or an acceptor material to get a p-doped and a n-doped material.

To create a solar cell, a p-n junction is needed. This is made by combining a p-doped and a n-doped material, and it will be created a depletion zone in the contact interface between the materials. In this depletion zone a small part of the p-doped material will naturalize the n-doped, and this area will not have free carriers. In addition, this area is polarized and the charge is creating an electric field which works as a

barrier for the holes and electrons. This barrier will be overflown with carriers if the voltage across the junction exceeds the threshold voltage of the barrier.

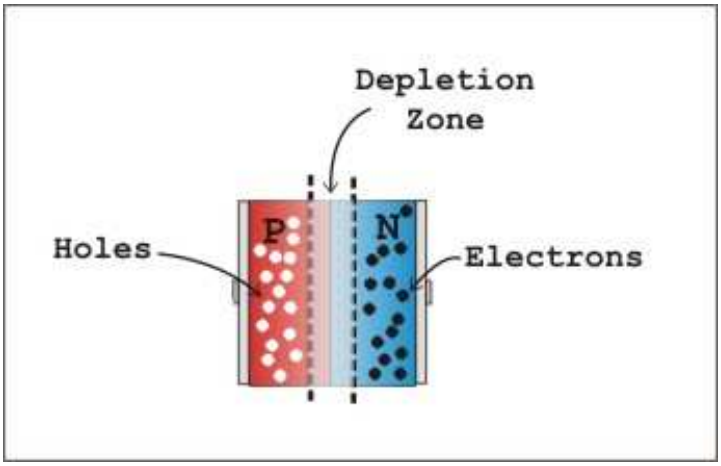

Figure 7.1: When p-doped and n-doped materials are combined, we get a p-n junction (Courtesy of Images SI Inc.)

A photovoltaic cell or a photo diode, is basically just a p-n junction. When the junction is illuminated, photons are hitting the depletion zone. A photon is the carrier of electromagnetic radiation of all wavelengths, including radiowaves, microwaves, infrared light, visible light, ultraviolet light, gamma rays and X-rays. When photons hit the photovoltaic cell, electrons are freed and attempt to unite with holes at the p-type side of the cell. The pn-junction is only conducting in one direction and only allows the electrons to move in one direction, towards the n-side. If then an external path for the electron to travel is provided, the electrons will flow through this path to the other side, the p-side, to unite with the holes. To be absorbed in this manner, the photon needs to have higher energy than the band gap of the semiconductor material. The gap for SI is about 1.15 eV, which corresponds to a wavelength of 1.08 µm. If the cell is exposed to light with shorter wavelength and greater energy than the energy needed for absorption, the remaining energy will be transformed to heat.

p-n junctions are the basic building blocks of almost every IC component, hence we can get photovoltaic effects, wanted and unwanted, in all these type of circuits. To prevent light from inducing photocurrents in a circuit, it is common to place it in an opaque housing. X-rays and other high energy radiation will still penetrate this, so it is very hard to eliminate the chance of photocurrents hundred percent, and the effect can cause a IC to malfunction.

Photodiodes is either used in photovoltaic mode, with zero bias, or

Material	Wavelength range (nm)
Silicon	190-1100
Germanium	400-1700
Indium gallium arsenide	800-2600
Lead sulfide	<1000-3500

Table 7.1: Common materials to make photo diodes from and the wavelength needed to create a current.

photoconductive mode, with a reverse bias. Photovoltaic mode is the basis for solar cells and in this mode the light causes a current across the diode, leading to a forward bias. This bias also induces co-called "dark current" in the opposite direction, which is a leakage current flowing through the photo diodes even when no photons are entering the device. The dark current includes photocurrent generated by background radiation and the saturation current of the junction.

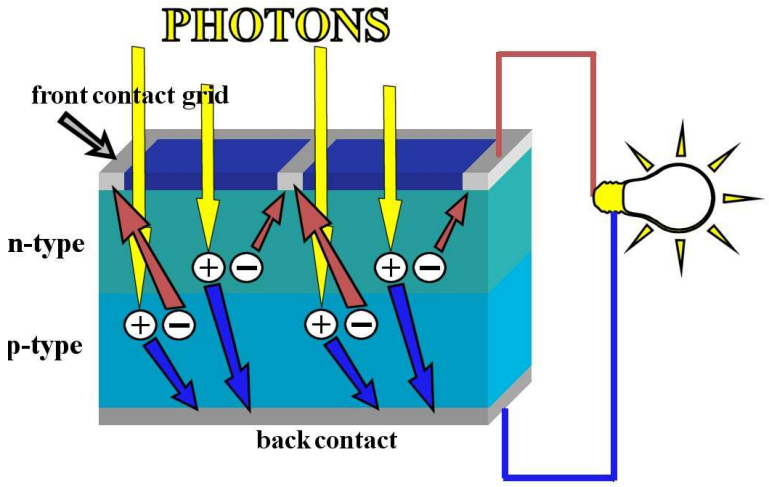

Figure 7.2: The way a photovoltaic cell work, also referred to as a photo diode. (Courtesy of SPECMAT Inc.)

Photoconductive mode diodes has a reverse bias and this bias induces a small current in the reverse direction. This is often called back current or saturation. The desired effect in photoconductive mode is enlarged depletion layer, which leads to expanded reaction volume, and stronger photocurrent. This increases the sensitivity to light and diodes in photoconductive mode have a lower capacitance and therefore a lower response time compared to diodes running in photovoltaic mode. A drawback with this mode is increased electronic noise from the diode.

If the reverse bias is high, the diode can operate with an avalanche

effect, and is called avalanche photodiodes. The carriers is then multiplied by an avalanche breakdown, and the diode will get an internal gain.

7.1.2 PIN diodes

A PIN diode is a diode with an intrinsic layer between the two doped semiconductor materials. The intrinsic layer is a wide, un-doped semiconductor region which expands the area available for absorption of photons. A challenge with the conventional diodes is the limited area of the depletion, and by using a PIN diode with a reverse bias, the bias increases the depletion region allowing a larger volume for electron-hole pair production, reduces the capacitance and thereby increasing the bandwidth. The PIN diode is suitable for many applications, especially the one demanding a wide dynamic range, high bandwith or both.

When inserting an intrinsic layer, some unwanted side effects will arise. The reversed bias, that the PIN diode must have, will introduce noise current which reduces the signal/noise ratio. For lower light applications the PN diode is preferred, as it can be used unbiased.

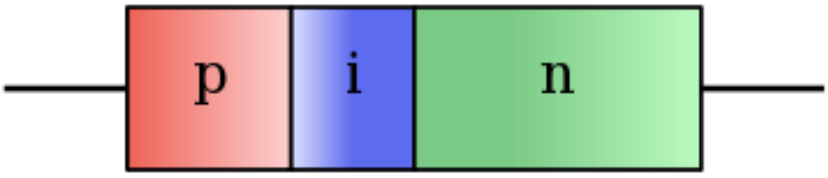

Figure 7.3: Photodiode with an un-doped intrinsic semiconductor material between the positive and negative doped layer.

7.1.3 Responsivity and quantum efficiency

The responsivity of a photodiode is important when calculating whether solar energy is enough for powering the system. This measurement is the ratio between the power of the incident light, which is photons, and the photocurrent, which is a result of converted electron-hole pair. The spectral responsivity has the units amperes per watt (A/W), and is a function of the photons' wavelength since the photons have different power at different wavelengths.

To calculate the percentage of photons hitting the photoreactive surface that actually will produce an electron-hole pair, we use Quantum Efficiency (QE). The QE of a sensor will then describe its response to different wavelengths of light. This is an important measure of a photoreactive device, as it also gives information on the current that a cell will produce when illuminated by a type of light. To do this, the quantum efficiency is

integrated over a chosen electromagnetic spectrum, i.e. solar light, and the current that a single cell will produce when exposed to this type of light can then be calculated.

In solar cell technology the External Quantum Efficiency (EQE), is the most interesting one. The EQE gives information on how much current obtained outside the device per incoming photon.

$$\mathrm{EQE} = \frac{\text{electrons/sec}}{\text{photons/sec}}$$

$$\mathrm{EQE} = \frac{\text{current/(charge of 1 electron)}}{\text{(total power of photons)/(energy of one photon)}}$$

The equation above shows that the external quantum efficiency both depends on the absorption of light and the collection of charges. When a photon has been absorbed and it has generated an electron-hole pair, these charges must be separated and collected at the junction. To increase the quantum efficiency and then also the current, is important to use materials that prevent recombination of charges.

7.2 Kinetic energy

Another potential energy source is the energy of movement, so called kinetic energy. When harvesting solar energy, certain conditions are required and the same applies for kinetic energy. Instead of available illumination, vibrations are needed and a system powered by convertion of kineticenergy to electric power will only be suitable for some applications. Even with a limited field of usage, it is worth looking into as RFID technology can be used in various surroundings, i.e. tagging lifestock and pets with tags powered from their movements or body energy.

7.2.1 MEMS-generators

Micro Electrical Mechanical Systems (MEMS) are systems made in micro scale or smaller, with mechanical parts working among with the electronics. These tiny mechanical systems are commercially used, i.e. in the car industry as accelerometers in airbags, as pressure sensors in medicine and to deposit the ink in printers.

The advantage with this technology is that movable, mechanical parts have characteristics that ordinary CMOS technology do not have, and can harvest from kinetic energy. Generators made with MEMS technology are still mostly at the research stage, but some implementations are on the market. One of the most promising available is the "electromagnetic micromachined silicon generator" researched at the University of Southampton and developed by Perpetuum Ltd. [Beeb 04].

This generator is made on a silicon base with a coil in the middle, along with four magnets. The coil is located between the 4 magnets such that the flux lines and the direction of motion are perpendicular to the coil windings. The coil is attached on a silicon cantilevered paddle, which is designed to vibrate laterally in the plane of the wafer. When the magnets and the coil are moving relative to each other, current is induced in the coil. When reaching the resonance frequency the paddle will get the maximum amplitude, hence the largest output voltage. The generator described is less than 1 mm^2 and output voltages of 760 mV (unloaded) is reported. With 100 kΩ load, the generator can deliver close to 2 mW at 12.6 kHz [Beeb 04]. These results are achieved at perfect conditions.

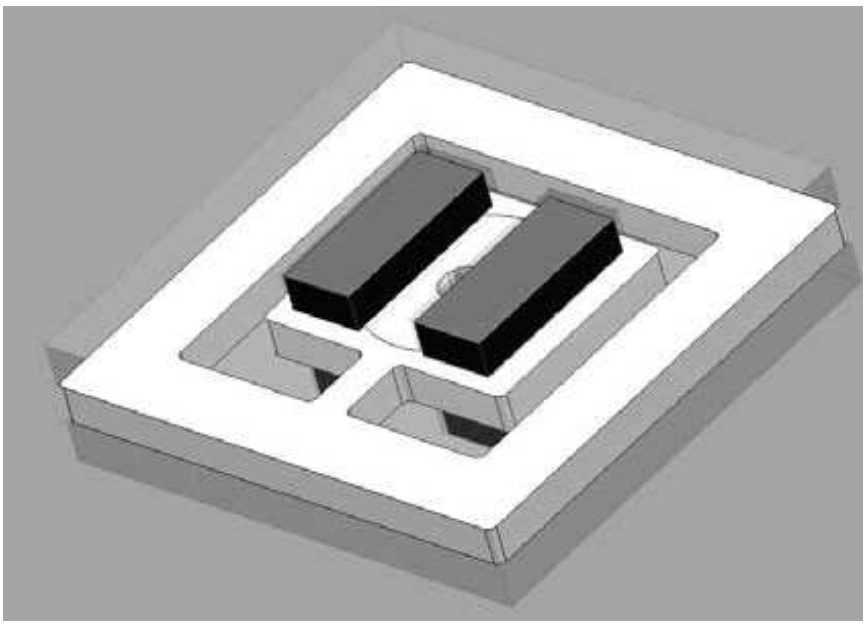

Figure 7.4: Electromagnetic micromachined generator. (Courtesy of Perpetuum Ltd.)

Combined with a CMOS RFID tag, a generator like this can partly or maybe even completely power the tag, given the right conditions. These conditions are some sort of movement when operating, causing the generator to oscillate, but at the same time not expose the generator to an amount of shocks causing the generator paddle to break.

7.3 Thermoelectric energy

Everywhere it is illumination, movement or heat, energy is also present. Heat can, i.e. as known from steam engines, be transformed into some other kind of energy, but when a very high temperature is not present, the

temperature differences can also be used to produce electrical energy. To be dependent of temperature differences or changes to power a RFID tag, strongly limits the commercial use, but still, it is a energy source to consider when selecting a technology. One example is measuring devices/implants in medicine, mounted on human skin, where a temperature difference exists between the two surfaces of the device.

Thermoelectric devices are in the simplest form just converters which directly convert temperature differences to electric voltage and vice versa. A thermoelectric device creates a voltage when there is a different temperature on each side, and if a voltage is applied, the device creates a temperature difference. The effect can be used to measure temperatures, to cool or heat objects or to generate electricity. Thermoelectrics are very convenient to use in temperature controllers, as the direction of heating and cooling is determined by the sign of the applied voltage.

The three effects within thermoelectrics are called the Seebeck effect, the Peltier effect and the Thomson effect. The Thomson effect describes the heating or cooling of a current-carrying conductor with a temperature gradient and the Peltier describes the conversion of electric current to heat, so the only interesting effect in this context is the Seebeck effect, which describes conversion from temperate to electric current.

7.3.1 Thermoelectrics - The Seebeck effect

In 1821 Thomas Johann Seebeck discovered the thermoelectric effect when he joined two wires of dissimilar metals, copper wire and bismuth wire, to form a circuit. He connected the wire ends to each other to form two junctions, and unaware of the consequences, he heated one junction to a high temperature. He discovered then if the other junction remained at a cooler temperature, a magnetic field was observed around the circuit of different temperatures [Seeb 08]. The discovery was then explained only by the term thermomagnetism, and the generation of electrical current was not described until some year later.

The Seeback effect is now described as a voltage that is created when a temperature difference is present between two different metals or semiconductors. This causes a current to flow if they form a complete loop and the voltage created is of the order of several μV per degree difference. This is called thermopower, even if it is voltage and not electric power that is measured. Thermopower has the units of V/K and a good thermoelectric material has thermopower of hundreds of microvolts per kelvin.

When applying a temperature difference in the setup shown in figure 7.6 on page 81, the difference will cause charged carriers, electrons or holes, in the semiconductor material, to diffuse from one side to the other. The moving charged carriers will leave behind oppositely charged nuclei

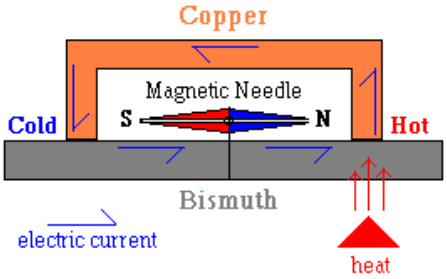

Figure 7.5: The setup Seebeck used to discover the thermoelectric effect. (Courtesy of Institute of Chemistry, University of Jerusalem)

at the other side of the circuit. Hot carriers diffuse from the hot end to the cold end, because of a lower density of hot carriers at the cold end, and visa versa. In a semiconductor material the electrons in the n-type element will flow toward the cooler region, and the holes in the p-type element will flow in the direction of the current.

This will give rise to a thermoelectric voltage, since the electrical potential created in this process can be withdrawn from the circuit. This potential will only build up to a certain level and reach a maximum when an equal amount of charged carriers are drifting back to the hot side as a result of equilibrium of the electric field. To increase this maximum value, the temperature difference must be increased. When the electric field reach thermodynamic equilibrium, the heat in the material will be distributed evenly throughout the conductor, and this movement of heat, which really is carriers, is called a heat current.

If the temperature difference of the conductor ends is kept constant relative to each other, there is a constant diffusion of carriers and a constant heat transfer. In theory the rate of diffusion of hot and cold carriers in opposite directions is equal, hence there would be no change in charge. This will not be the case, since the diffusing carriers are scattered by imperfections in the material, lattice vibrations and imperfections, and the hot and cold carriers will diffuse at different rates if the scattering is energy dependent. An electrical current will then flow as the difference in diffusing rate creates a higher density of carriers at one end, and the positive and negative charges produces a potential difference.

The thermopower of the material used, depends of the crystal structure of the material and the temperature. The thermopower of metals is typically quite small, because most metals have half-full bands. This will result in electrons and holes cancelling each other out, and the induced thermoelectric voltage will be small. Semiconductors however have larger thermopower if doped, because of overload of one type of charged carriers, hence can have large positive or negative values of the thermopower.

Similar to photoelectric effects. This positive or negative sign depends on the charge of the dominating carriers in the material. The thermopower of the material depends also on impurities, imperfections, structural flaws and changes. The electric field created by the circuit opposes the uneven scattering of carriers, and the equilibrium of the field is reached when net number of carriers in one direction are cancelling out net number of charges in the opposite direction of the electric field.

The thermopower of a material is defined as

$$S = \frac{\Delta V}{\Delta T} = \frac{E}{\nabla T}$$

where V is the thermoelectric voltage, T is the temperature and E the electric field. This is called the absolute thermopower, but is not always of interest. This is because when measuring the voltage, the temperature gradient will induce a thermoelectric voltage across one leg of the measurement electrodes. The measured thermovoltage will then have a contribution from this voltage, and can more accurately be written as

$$S_{AB} = S_B - S_A = \frac{\Delta V_B}{\Delta T} - \frac{\Delta V_A}{\Delta T}$$

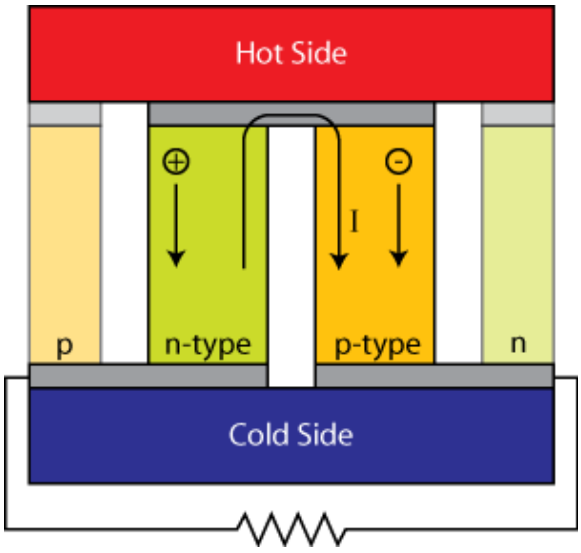

Figure 7.6: A thermoelectric element. (Courtesy of Case Western Reserve University)

The thermoelectric power and electrical conductivity maximizes somewhere between a metal and semiconductors. Good thermoelectric materials are typically heavily doped semiconductors or semimetals with carrier concentration of 10^{19} to 10^{21} carriers/cm^3. The materials with only one

type of carriers, have the largest Seebeck effect, because mixed n-type and p-type conduction will lead to opposing effects and low thermopower. By looking at figure 7.7, we can see the thermopower of different materials and as described above, the material with the largest thermopower is a mix of metal and semiconductor.

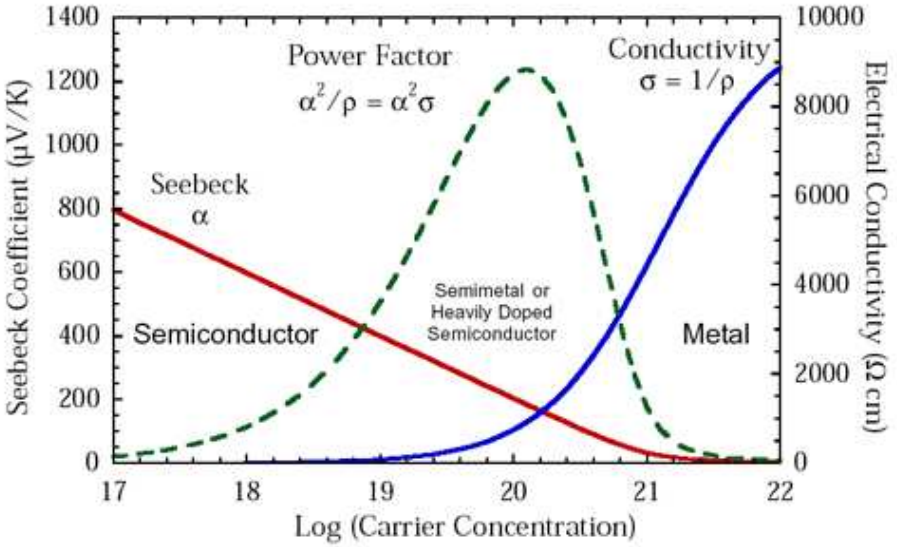

Figure 7.7: The thermopower of different materials. (Courtesy of California Institute of Technology)

7.4 Practical use of alternative energy sources

We have now taken into consideration three different energy sources not commonly used in wireless identification. As we can see that it is hard to power a RFID tag based sources like temperature, movements or light. Mostly because of the environmental issues like the need of a constant temperature difference, but under the right conditions these sources can be used with success. Another problem is the space requirements. To make a practical implementable system with thermoelectric powering, quite large elements is needed in order to maintain the temperature difference and get a high output voltage.

A photodiode or a Seebeck element, limited to a few mm^2, will only produce voltages of a few millivolts when loaded, typically a few microwatts, hence they will not deliver enough current alone to power a complete system on a tag. MEMS generators are promising devices, and at good conditions, a fair amount of power can be delivered, especially when multiple devices are used. The drawback will be the constant need

of movements, risk of shock damages and they will occupying a large area. Photo diodes is probably the most suitable technology, of these three, for wireless identification, regarding space and effect, but then the problem with illumination will come into play.

Figure 7.8: Commercial use of thermoelectric effect, photo cells and kinetic energy.

To include solar and illumination power on a RFID tag as described in the previous chapters, the cells have to be implemented in CMOS technology. Since regular CMOS transistors is made from doped silicon, integration of photo cells in a standard CMOS processes is a simple task. Solar technology can also be included in the RFID tag as an external component on the side of the chip, but this will make the fabrication of the tag more expensive and complex. Silicon photodiodes are commercially available, both as PN and PIN, and by looking at datasheets from big commercial actors in the semiconductor industry, like Hamamatsu and OSI optoelectronics, we can see that photodiodes and cells exists in a variety of sizes, materials and output specifications. If the selection is narrowed down to semiconductor devices smaller than 1 mm^2, the responsivity is in the range 0.2 - 0.7 A/W, and dependent of the wavelength of the light used to illuminate the cell. The output of a photocell arrangement can be further enlarged by the use of a chargepump, like the one in chapter 5 on page 41. The chargepump can either be placed after the photodiodes to boost the output ([Liu 01] and [Ochi 05]), or the diodes can be integrated in the pump itself.

Another key issue is the costs of producing the tag. When using thermoelectric elements in small fridges, mechanical generators in wrist watches or photodiodes to power calculators this factor can be adjusted to a reasonable level. When designing a passive RFID tag, you have to keep in mind mass production and the possibility of single use. Both the size and costs of a single tag have to be minimized.

The conditions that have to be right for the harvesting to succeed, limits the use significantly, but a combination of several energy sources can be

imaginable to use on a wireless tag. A scenario can be a illuminated tag, with photocells charging the capacitors together with chargepump technology. Either as a backup system if the wireless signal gets weakend, or simultaneously to create a greater power supply for the on-chip transmitter. But for now, these three energy sources discussed are limited to larger applications, like the one in figure 7.8.

Chapter 8

Concluding remarks

The power issues in modern IC industry are one of the grand challenges of the International Technology Roadmap for Semiconductors [ITRS 07], but when the biggest concern elsewhere is to reduce temperature at small areas, the main challenge for passive wireless technology is to get a hold of the energy. As we have seen throughout the last chapters, the energy is available, but it is not a trivial operation to use it. Even wireless systems, like RFID systems, are commercially ready, the potential for expanding the use of passive tags are huge. According to the Santella Consulting, from 2006 to 2007, the total spending on RFID hardware in the U.S. increased from $607 to $875 billion U.S. dollars. A growth of 30%. This is much due to larger systems, more complex readers and an massive market expansion, but still, the costs can, and should, be dramatically reduced. If the power harvesting issues are improved, together with the transmission methods, not only reduces cost, but also improves performance.

Tags only powered by RF signals means no battery, extended lifetime and lower cost. It is promising, but the technology has some steps to take before these kind of tags are able to replace semi-active tags. In many ways we can say that RFID technology is a premature technology growing up to fast, and companies world wide are using billions of dollars on a technology, which they know little or nothing about the potential of. The answer to this question is not presented in this thesis, but with this work it has been proved that energy from a RF signal is a promising source.

This thesis has presented different aspects of power harvesting, implemented a charge pump in CMOS technology and reviewed a selection of alternative energy sources. The work started with an introduction, and then narrowed the research down to power harvesting and circuit design. This was followed by a implementation of a charge pump in CMOS, simulations and measurements. At the end of the thesis, three well known, but alternative energy sources was reviewed. Alternative, because they are common in lager applications, but not commonly used at chip level designs. The

results of this review have been various, but have given an understanding of what is practical doable and what is, for now, at an experimental level.

The novel diode models and couplings have been successful, and the results from chip measurements have been satisfying, close to simulation results. This confirms the hypothesis presented at the beginning of this thesis, that RF signals can be used to power a passive tag. The practical range of this energy is yet to be known, as extensive antenna-to-chip measurements are not included in this thesis.

8.1 Future work

To take the circuit design of the charge pump further, there are some quite clear fields of improvement. Some is regarding the pump itself, and other to test the charge pump as a part of a complete system.

- An important improvement that has to be done, is to reduce reflections and increase power transmission from the signal source or antenna to the circuit. This have to be done by adding improved impedance matching.
- The second aspect is more research of antennas and air transmissions. This is important in order to test the stability of the pump and ability to generate a DC voltage from a unstable AC signal.
- To find out how the pump is working in a system, the pump should be tested with a low power transmitter, and measurements should be done to find required input signal at different transmission ranges and environments.
- To improve the pump further, the diodes can be replaced with pass-gates. These can be controlled by a control circuit, that will switch the transistors on and off. This can be done to test the maximum performance of the pump, but can also be an interesting design if successfully made.
- The charge pump has until now only be tested at certain frequencies. These were selected due to their availability, but it does not mean that other frequencies not can be used. This will of course affect the antenna size and air loss, and also transmission regulations.
- Boost converting is another voltage boosting method worth looking more into. If the boosted converted DC signal is used to power a UWB-IR transmitter, the boosted signal can be “shot” into a pulse or a pulse train. Since the output from the boost converter is high voltage, but low current, it is still suitable for a pulse transmitter. This might

not be a good idea if used together with a conventional AM or FM transmitter, because the amount of output power would probably be to low to generate a steady carrier frequency.

- In order to test the three alternative energy sources and not just rely on measurements from articles, measurements of these are interesting. This can be implementations in CMOS together with the charge pump, or measurements of devices made by others. In either case, testing photovoltaics, MEMS generators and thermoelectrics as energy sources together with RF signals could be of interest, and will give a better insight to these energy forms.

Chapter 9

Acronyms

AC Alternating Current

ADC Analog to Digital Converter

ADS Active Denial System

AM Amplitude Modulation

ANA Article Number Association

ASK Amplitude Shift Keying

CMOS Complementary Metal-Oxide Semiconductor

CBI Cross-Band Interrogation

CCTV Closed Circuit Television

CEN European Committee for Standardization/Comité Européen de Normalisation

DC Direct Current

EAN European Article Numbering

EAS Electronic Article Surveillance

ECCC Electronic Commerce Council of Canada

EHF Extremely High Frequency (30-300 GHz)

ENG Electronic News Gathering

EPC Electronic Product Coding

EU European Union

EQE External Quantum Efficiency

FET Field Effect Transistor

FCC Federal Communications Commission

FSL Free Space Loss

FM Frequency Modulation

FSK Frequency Shift Keying

FWA Fixed Wireless Access

GSM Global System for Mobile communications

IC Integrated Circuit

IEC International Electrotechnical Commission

IEEE Institute of Electrical and Electronics Engineers

IFF Identification Friend or Foe

IR Impulse Radio

ISM Industrial, Scientific and Medical

ISO International Standards Organization

ITU International Telecommunication Union

JLCC J-Leaded Chip Carrier

LAN Local Area Network

MEMS Micro Electrical Mechanical Systems

MIT Massachusetts Institute of Technology

MOS Metal Oxide Semiconductor Field Effect Transistor

MPT Microwave Power Transmission

NASA National Space Agency

NMOS n-channel MOS

NPT Norwegian Post and Telecommunications Authority

PCB Printed Circuit Board

PMOS p-channel MOS

PSK Phase Shift Keying

QE Quantum Efficiency

RAF Royal Airforce

RCA Radio Corporation of America

RF Radio Frequency

RFID Radio Frequency Identification

SAW Surface Acoustic Wave

SHF Super High Frequency (3-30 GHz)

SMA SubMiniature version A

SPS Solar Power Satellite

SSP Space Solar Power

UCC Uniform Code Council

UHF Ultra High Frequency (0.3-3 GHz)

UWB Ultra Wide Band

WLAN Wireless Local Area Network

Appendix A

IC

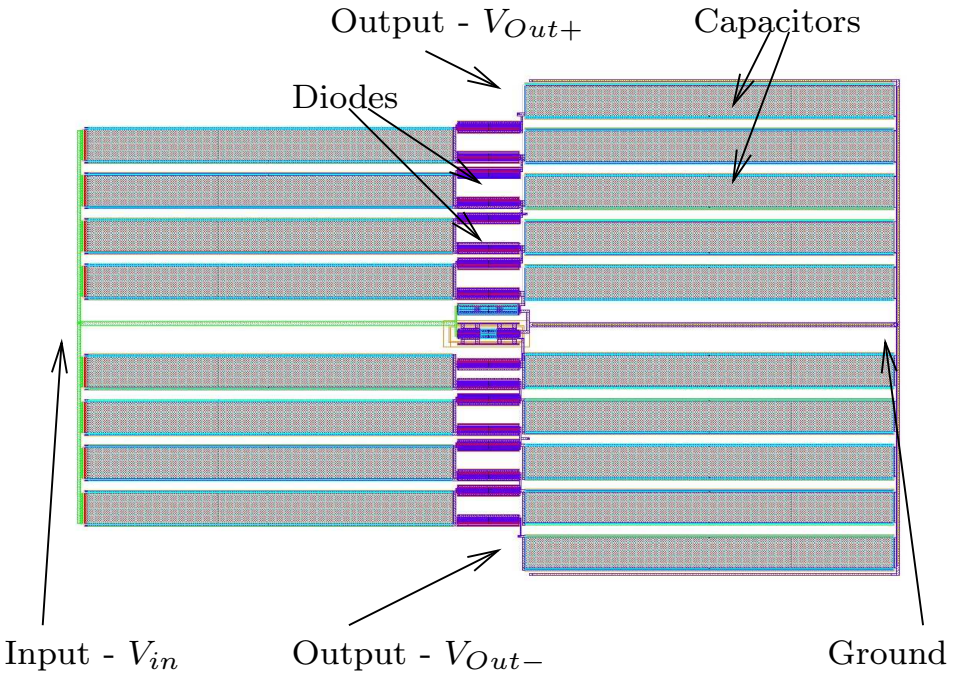

Figure A.1: Layout of the charge pump

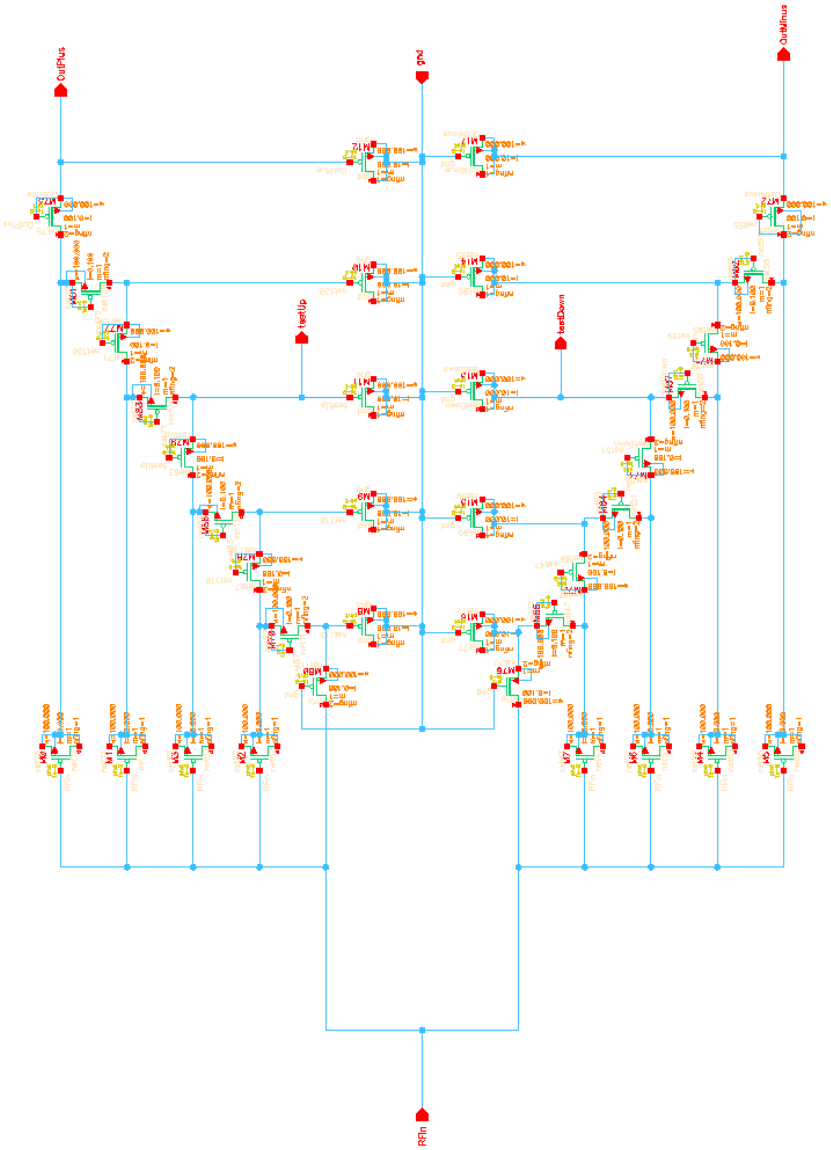

Figure A.2: Schematic of the charge pump

Appendix B

PCB

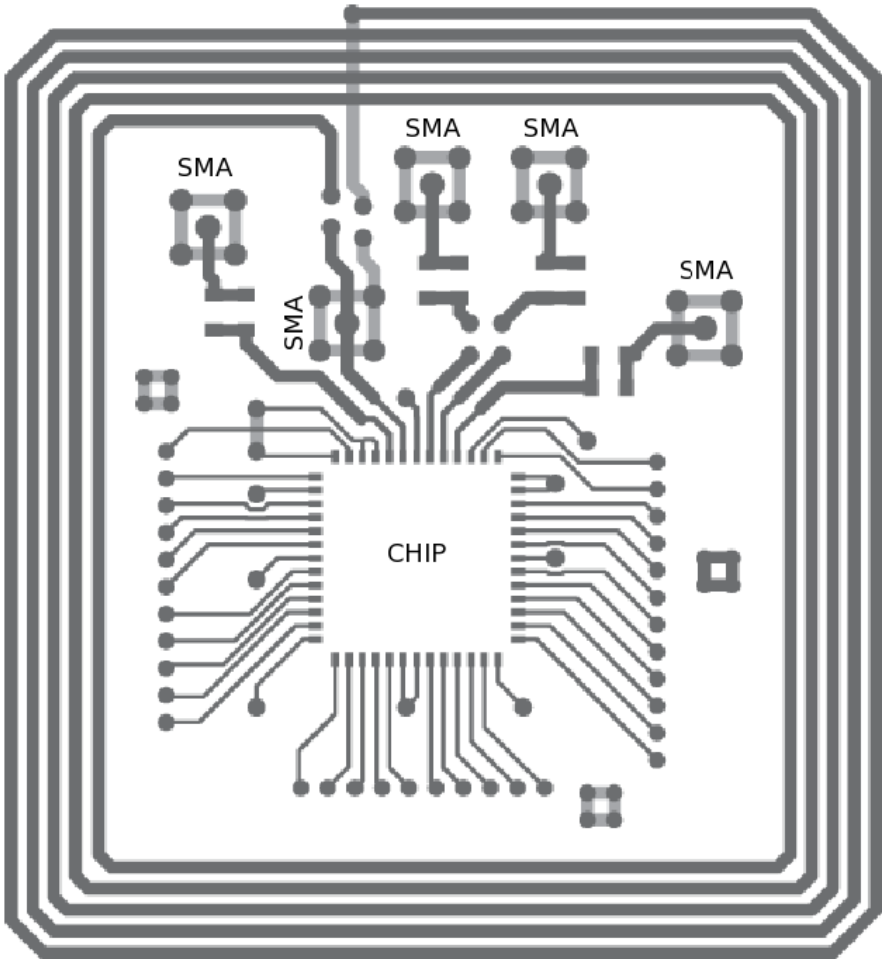

Figure B.1: Layout of the PCB

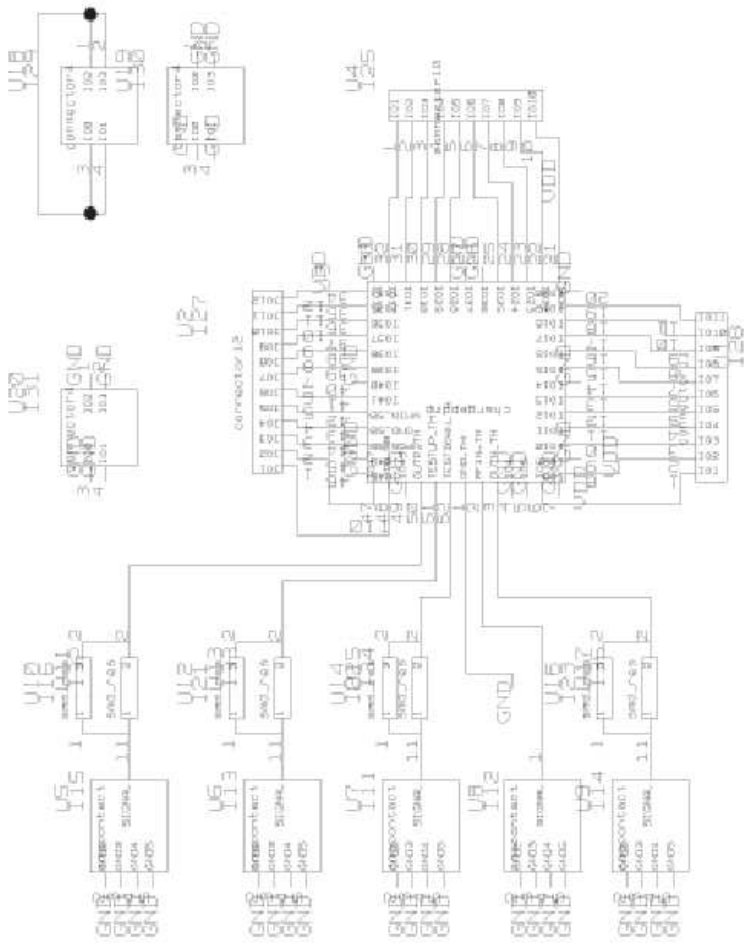

Figure B.2: Schematic of the PCB

Bibliography

[Alst 08] H. P. Alstad and S. Aunet. "Three Subthreshold Flip-Flop Cells Characterized in 90 nm and 65 nm CMOS Technology". In: *Proceeding of IEEE DDECS*, pp. 8–11, 2008.

[Arms 36] E. H. Armstrong. "A Method of Reducing Disturbances in Radio Signaling by a System of Frequency Modulation". *Proceedings of the IRE*, Vol. 24, No. 5, pp. 689–740, May 1936.

[Beeb 04] S. P. Beeby, M. J. Tudor, E. Koukharenko, N. M. White, T. O'Donnell, C. Saha, S. Kulkarni, and S. Roy. "Micromachined Silicon Generator for Harvesting Power from Vibrations". *The 4th International Workshop on Micro and Nanotechnology for Power Generation and Energy Conversion Applications (PowerMEMS 2004)*, 28-30th November, Kyoto, Japan 2004.

[Bene 04] M.-G. D. Benedetto and G. Giancola. *Understanding Ultra Wide Band Radio Fundamentals. Communications Engineering and Emerging Technologies Series*, Prentice Hall, June 2004.

[Brow 65] W. C. Brown. "Experimental Airborne Microwave Supported Platform". Tech. Rep., Report nr. 0529474, December 1965.

[Case 82] M. T. Casey. "Nicholas Callan - priest, professor and scientist". *Physics Education, Institute of Physics Publishing*, Vol. 17, No. 5, pp. 224–234, 1982.

[Chaw 07] V. Chawla and D. S. Ha. "An Overview of Passive RFID". *IEEE Applications & Practice*, September 2007.

[Curt 05] J.-P. Curty, N. Joehl, C. Dehollain, and M. J. Declercq. "Remotely Powered Addressable UHF RFID Integrated System". *IEEE J. Solid-State Circuits*, Vol. 40, No. 11, pp. 2193–2202, November 2005.

[Dick 76] J. F. Dickson. "On-chip high-voltage generation in NMOS integrated circuits using an improved voltage multiplier technique".

IEEE J. Solid-State Circuits, Vol. SC-11, No. 3, pp. 374–378, June 1976.

[ERC 04] European Radiocommunications Committee (ERC). *ERC Report 25 - European Common Allocation Table*, May 2004.

[Fano 48] R. M. Fano. "Theoretical Limitations on the Broadband Matching of Arbitrary Impedances". Tech. Rep. 41, Research Laboratory Of Electronics, Massachusetts Institute Of Technology, January 1948.

[Fara 08] "Faraday, Michael". Encyclopædia Britannica Online, April 2008. http://www.britannica.com/eb/article-9109756.

[Fink 03] K. Finkenzeller. *RFID Handbook: Fundamentals and Applications in Contactless Smart Cards and Indentification*. John Wiley and Sons, 2 Ed., 2003.

[Grap 72] *Graphical symbols for electrical power telecommunications and electronics diagrams*. The British Standards Institution, 1972. BS3939 - Section 27.

[ITRS 07] ITRS. "International Technology Roadmap For Semiconductors". 2007.

[John 97] D. Johns and K. Martin. *Analog Integrated Ciruit Design*. John Wiley & Sons, Inc, 1997.

[Kart 03] U. Karthaus and M. Fischer. "Fully Integrated passive UHF RFID transponder IC with 16.7-μW minimum RF input power". *IEEE J. Solid-State Circuits*, Vol. 38, No. 10, pp. 1602–1608, October 2003.

[Land 01] D. J. Landt. "Shrouds of Time - The history of RFID". *AIM - Association for Automatic Identification and Data Capture Technologies*, pp. 11–17, 2001.

[Lees 00] H. Leeson, P. Hansell, J. Burns, , and Z. Spasojeviç. "Demand for use of the 2.4GHz ISM Band Final Report". Tech. Rep., Spectrum Management Advisory Group, Aegis Spectrum Engineering, July 2000.

[Liu 01] W.-J. Liu, O. T.-C. Chen, L.-K. Dai, P.-K. Weng, K.-H. Huang, and F.-W. Jih. "A CMOS photodiode model". *Behavioral Modeling and Simulation, 2001. BMAS 2001. Proceedings of the Fifth IEEE International Workshop on*, pp. 102–105, 2001.

[Ludw 00] R. Ludwig and P. Bretchko. *RF Circuit Design: Theory and Applications*. Prentice Hall, January 2000.

[Mars 03] K. M. Marsden, D. S. Ha, J. R. Armstrong, and S. Raman. *A Study of a Versatile Low Power CMOS Pulse Generator for Ultra Wideband Radios*. Master's thesis, Virginia Polytechnic Institute and State University, December 2003.

[Mill 87] J. Millman and A. Grable. *Microelectronics*. McGraw-Hill Book Co., second edition Ed., 1987.

[Moen 06] H. Moen. *UWB Impulse Radio for RFID*. Master's thesis, Department of Informatics, University of Oslo, August 2006.

[Mors 08] "Morse, Samuel". Encyclopædia Britannica Online, April 2008. http://www.britannica.com/eb/article-9053834/.

[Ochi 05] S. Ochi and N. Zommer. "Solar cell device having a charge pump". *US Pantent Publication*, March 2005.

[Raby 70] O. Raby. *Radio's First Voice: The Story of Reginald Fessenden*. MacMillan of Canada, Toronto, 1970.

[RFID 07] RFID Innovasjonssenter AS. *RFID i Næringslivet, status og trender*, GSK Konferansesenter, October 2007.

[Seeb 08] "Seebeck, Thomas". Encyclopædia Britannica Online, April 2008. http://www.britannica.com/eb/article-9066564.

[Shep 04] S. Shepard. *RFID. Networking Professional*, McGraw-Hill, 1 Ed., August 2004.

[Stoc 48] H. Stockman. "Communication by Means of Reflected Power". *Proceedings of the IRE*, pp. 1196–1204, October 1948.

[Stru 85] J. W. Strutt and B. Rayleigh. "On waves propagating along the plane surface of an elastic solid". In: *London Mathematical Society Proceedings*, pp. 4–11, 1885.

[Stur 08] "Sturgeon, William". Encyclopædia Britannica Online, April 2008. http://www.britannica.com/eb/article-9070045.

[Why 59] "Why Radio Amateurs Are Called "Hams"". Florida Skip Magazine, 1959.

[Yao 05] Y. Yao, Y. Shi, and F. F. Dai. "A Novel Low-Power Input-Independent MOS AC/DC Charge Pump". *IEEE International symposium on Circuits and Systems, ISCAS*, Vol. 1, pp. 380–383, 23-26 May 2005.

[Zhou 03] F. Zhou, D. Jin, C. Huang, and M. Hao. "Optimize the power consumption of passive electronic tags for anti-collision schemes". *ASIC, 2003. Proceedings. 5th International Conference on*, Vol. 2, pp. 1213–1217, October 2003.

Paper

Power Harvesting Circuits in 90 nm Technology

Submitted for conference review.

Power Harvesting Circuits in 90 nm CMOS

Trygve K. Halvorsen, Håkon A. Hjortland and Tor Sverre "Bassen" Lande
Dept. of Informatics, University of Oslo, Norway
E-mail: {trygvekh, haakoh, bassen}@ifi.uio.no

***Abstract*— The purpose of this paper is to explore power harvesting capabilities in nanometer technology. Novel charge pump improvements using the back-gate or well of MOS devices improve efficiency as well as sensitivity. The proposed circuits are implemented in 90 nm CMOS. Measured performance will be provided.**

I. Introduction

Power harvesting integrated as part of a standard CMOS technology would be useful in several applications. Typically in RFID tags, inductive power harvesting is used [1] requiring fairly large, external inductors and working primarily in near field. Exploring electromagnetic waves over longer distances is tempting and might even recover radio waves from devices like mobile phone or wireless LAN. To some extend the downsizing of technology is reducing power requirements, but reduced supply voltage is limiting the controllable on-chip voltages to less than 1 V. As circuits, both digital and analog, are exploring subthreshold transistor operation [2], power harvesting circuit elements for fine-pitch CMOS technology is worthwhile exploring. In this paper we will present the fundamental charge pump circuit and explore design improvements for better efficiency.

II. Charge Pump Circuits

The original Dickson charge pump [3] circuit is shown in Fig. 1.

The major building blocks required are capacitors and rectifying elements, i.e. diodes. As capacitors are readily available in CMOS, the challenging element is the rectifier element. The first order operation of the original Dickson charge pump is the two-phase clock that is capacitively lifting the node charge on the rising edges through the diode, while the diodes are preventing the charge to leak back on the negative clock

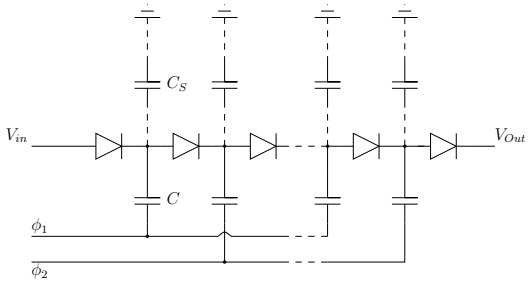

Fig. 1. The original Dickson charge pump

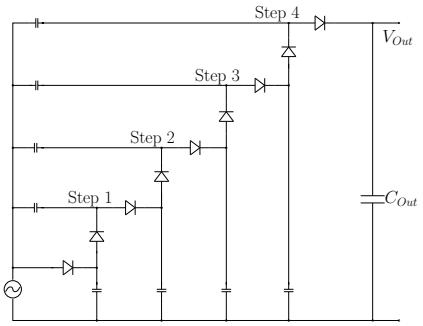

Fig. 2. Four-step cascode charge pump

transition. For power harvesting a single phase architecture is necessary like the one in Fig. 2.

A single AC source is rectified and charge is built up using capacitors and diodes [4]. Our implementation in silicon is based on the circuit topology of Fig. 2. By exploring the design space of modern technology, some reasonably effective circuits are feasible, and in the following we will explore modern CMOS technology for improved charge pump performance.

III. CMOS Technology Options

The optimal rectifying element would be a device with low or no resistance when forward biased and with no conductance or infinite resistance when reverse biased. The normal diode forward biasing voltage of 0.7 V makes junction diodes unsuitable for power harvesting. Incoming antenna signals are normally $<$100 mV and the forward biasing voltage must be within the range of the received signal. The substitute of a junction diode in CMOS is a diode-connect MOS transistor. In addition, a number of different threshold voltages are available as different devices; low, standard and high threshold. Low gate leakage devices are also available, but sometimes the transconductance is reduced.

As shown in Fig. 3, the differences between the threshold voltages are significant when comparing the 3 different devices of 90 nm MOS transistors. In order to make the charge pump maximum efficient, the threshold voltages of the diodes have to be low when pumping the voltage in order to get the voltage drop minimized. On the other hand when pushing the charge further on, at the negative half-period of the input, a high threshold is needed in order to reduce the leakage in the reverse direction of diode as much as possible. Benefits of

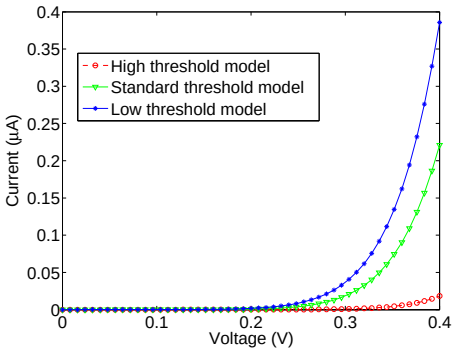

Fig. 3. MOS transistors diode-connected (low, standard and high threshold).

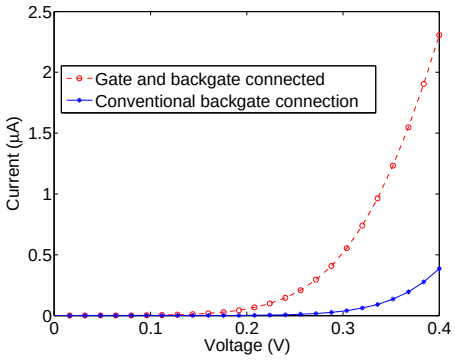

Fig. 4. A classically diode connected PMOS transistor (low threshold device) compared to one with gate and backgate connected.

increased forward current outweighs the detrimental effects of the increased reverse current.

Another option of modern CMOS processes is triple well devices. With low supply voltages, the well potential may be explored for both dynamic threshold adjustment and improved efficiency. First we can take a look at the following equation [5],

$$V_{th} = V_{th_0} + \gamma \left(\sqrt{V_{sb} + |2\phi_F|} - \sqrt{|2\phi_F|} \right) \quad (1)$$

where γ is the body effect parameter, $2\phi_F$ is the surface potential, and V_{th_0} is the zero bias threshold voltage. V_{sb} is a parameter that can be altered to achieve a lower V_{th}. This is done by connecting the back-gate/bulk contact to a different potential, hence causing a reversed body effect. The bulk connection can be thought of as a second gate, and can alter the threshold.

With this knowledge in mind, a charge pump based on the one in Fig. 2 was designed.

IV. CMOS High Sensitivity Charge Pump

The charge pump can be described as a series of steps, and one step of the pump is shown in Fig. 5.

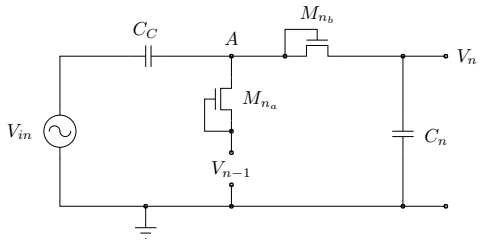

Fig. 5. One step of the charge pump

This charge pump works as follows; the positive half period of the input will charge capacitor C_n and the diode coupled transistor will prevent the current flowing back. At the throughs of the input sine wave,

$$V_A = V_{n-1} - V_{th}. \quad (2)$$

At the peaks, this voltage rises $2 \cdot V_{in}$, and reaches

$$V_A = V_{n-1} - V_{th} + 2 \cdot V_{in} \quad (3)$$

C_n will be charged to $V_A - V_t$:

$$V_n = V_{n-1} + 2 \cdot V_{in} - 2 \cdot V_{th} \quad (4)$$

Each step of the charge pump can not increase the pumped voltage more than two times the amplitude of the input voltage minus two times the threshold voltage of the transistors. If the low-threshold models in the 90 nm technology are used, the diode threshold voltage will be 0.18 V. This means that, with no modifications to the circuit, the input amplitude must exceed 0.18 V to get the charge pump to pump voltage through the steps towards the last capacitor. With the backgate connection proposed in section III, the charge pump can work at even lower inputs.

To maximize the output voltage in this circuit, there are two main factors; minimize the threshold voltage or increase the number of steps. Since increasing the number of steps will cause degradation of power and conversion efficiency and also increased circuit size, lowering the voltage drop of the transistors is the most efficient way to improve the charge pump.

If we take a look at the threshold voltage of a transistor in the triode region [5], we can see the relationship between the transistor current and W/L.

$$I_{ds} = \beta \cdot \left((V_{GS} - V_t) \cdot V_{DS} - \frac{V_{DS}^2}{2} \right) \quad (5)$$

$$\beta = \mu_n \cdot C_{ox} \cdot \frac{W}{L} \quad (6)$$

To ensure pumping at low input voltages we will need a low V_{th}, and to ensure that we are able to deliver as much current as possible, W/L and capacitors must be as large as possible without the capacitive load at the input of the circuit becoming too large. This can potentially be a problem in a

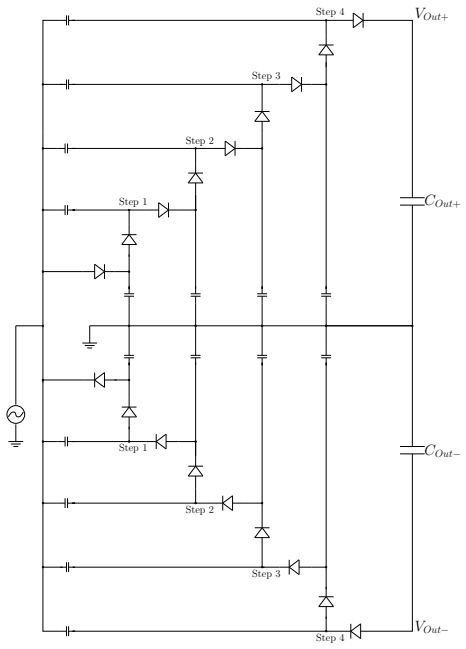

Fig. 6. Charge pump with both a positive and a negative output voltage

practical implementation, because the input source will then not be able to drive the charge pump.

Until now only a positive output voltage has been extracted from the charge pump, but by further developing the pump like in Fig. 6, it can give a negative output just as big as the positive [6]. By defining V_{Out-} as ground, the available output voltage will be doubled.

V. CMOS Charge Pump Simulations

The charge pump is simulated with 900 MHz and 2.45 GHz input, and the results are shown in Fig. 7(a) and Fig. 7(b). These two frequencies are used by GSM and WLAN, and in this range several unlicensed bands can be found [7], [8]. The amplitude of the input signal is 100 mV. At higher frequencies the load will affect the circuit more and more, and will have to be kept in mind in a practical scenario. The results are promising for use in low-power wireless systems that require low voltage DC supplies.

VI. Implementation in 90 nm CMOS

In Fig. 8 the layout of the chargepump is shown. It is arranged with the C_C capacitors on the left and the C_n capacitors on the right. The diodes are placed in the middle to avoid long wires. Two test outputs are placed in the middle of the pump for measuring purposes.

VII. Charge Pump Measurement Setup and Performance

In Fig. 9 the PCB is shown. The long production time for the process used (>6 months) has delayed our measurements.

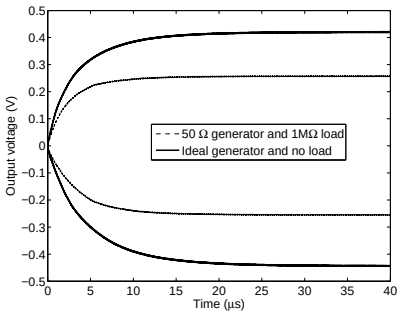

(a) 900 MHz

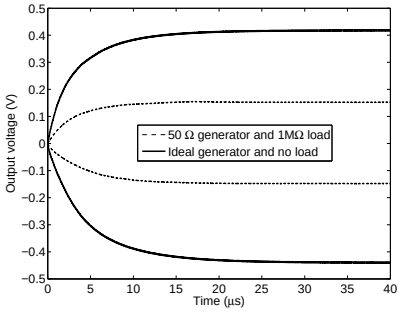

(b) 2.45 GHz

Fig. 7. Time development of charge pump output

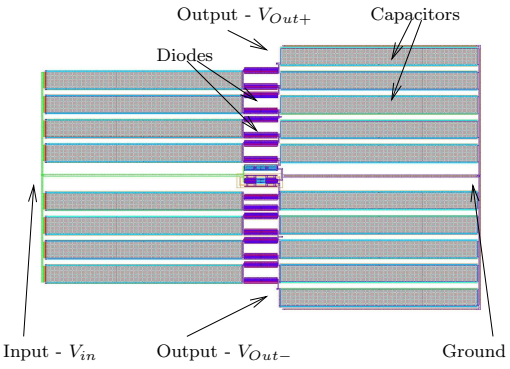

Fig. 8. Layout of the charge pump

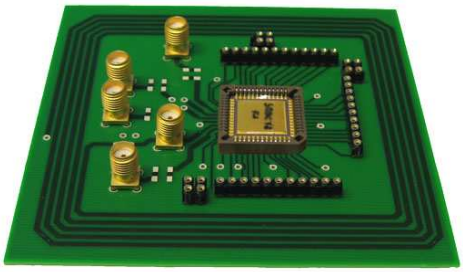

Fig. 9. The PCB with the chip mounted.

The results so far are good, and matches the simulations. In Fig. 10(a) and 10(b) the output as a function of input signal is shown. In Fig. 10(c) the output power at different input amplitudes and output voltages are shown. As we can see in Fig. 10(a), the symmetry in broken when V_{-} is below approximately 0.5 V. This is because the pad frame of the chip has diodes between the pads and ground to prevent overloading of the chip. This problem can easily be solved with use of a different pad frame. As Fig. 10(c) shows, the charge pump is promising regarding power. I.e. the pump need just around 300 mV input amplitude to generate 60 µW with 1 V DC output. This can be sufficient to power a pulse transmitter, as a wireless identification tag.

VIII. Conclusion

In this paper we have presented a high sensitivity charge pump suitable for power harvesting of reasonably small RF signals commonly emitted by wireless equipment. The novel exploration of the back-gate for improved performance indicates the feasibility of power harvesting in devices like RFID.

References

[1] K. Finkenzeller, *RFID Handbook: Fundamentals and Applications in Contactless Smart Cards and Indentification*, 2nd ed. John Wiley and Sons, 2003.

[2] W. M. Sansen, *Analog Design Essentials*, 1st ed. Springer, 2006.

[3] J. F. Dickson, "On-chip high-voltage generation in nmos integrated circuits using an improved voltage multiplier technique," *IEEE J. Solid-State Circuits*, vol. 11, no. 6, pp. 374–378, June 1976.

[4] U. Karthaus and M. Fischer, "Fully integrated passive uhf rfid transponder ic with 16.7-μw minimum rf input power," *IEEE J. Solid-State Circuits*, vol. 38, no. 10, pp. 1602–1608, October 2003.

[5] D. Johns and K. Martin, *Analog Integrated Ciruit Design*. John Wiley & Sons, Inc, 1997.

[6] J.-P. Curty, N. Joehl, C. Dehollain, and M. J. Declercq, "Remotely powered addressable uhf rfid integrated system," *IEEE J. Solid-State Circuits*, vol. 40, no. 11, pp. 2193–2202, November 2005.

[7] H. Leeson, P. Hansell, J. Burns, , and Z. Spasojevi, "Demand for use of the 2.4ghz ism band final report," Spectrum Management Advisory Group, Aegis Spectrum Engineering, Tech. Rep., July 2000.

[8] *ERC Report 25 - European Common Allocation Table*. European Radiocommunications Committee (ERC), May 2004.

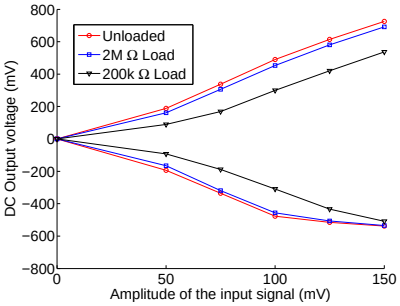

(a) DC output at 1 GHz

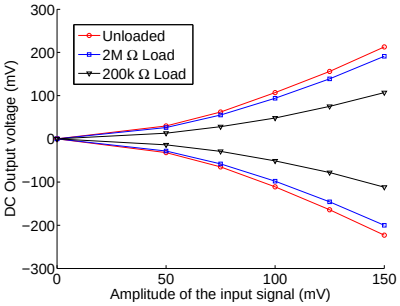

(b) DC output at 2.45 GHz

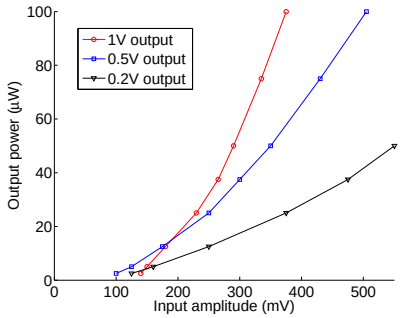

(c) Output power as a function of input and output voltages.

Fig. 10. Results of the measurements.